

# **DRAFT - Organic nitrogen in the Los Angeles atmosphere**

Authors

## **Abstract**

We report an inventory of nitrogen-containing organic compounds in the Los Angeles Basin in late August, 2021. Gas-phase multifunctional nitrogen-containing compounds are measured by chemical ionization mass spectrometry (CIMS) using the  $\text{CF}_3\text{O}^-$  reagent ion both with and without gas chromatography (GC) separation. We use a time-of-flight aerosol mass spectrometer (ToF-AMS) to quantify the abundance of nitrogen-containing organic compounds present on sub-micron particles. These nitrogen-containing organic compounds comprise a substantial fraction of non- $\text{NO}_x$  reactive nitrogen during the day and, together with nitrous acid (HONO), the vast majority during nighttime. Alkylnitrates produced in the oxidation of biogenically- and anthropogenically-derived alkenes dominate the budget, but nitroaromatics also make a significant contribution. The GC-CIMS observations illustrate that the nighttime alkyl nitrates are generated via reaction of alkenes with the nitrate radical and that the resulting nitrooxy-peroxy radicals react with both  $\text{HO}_2$  to form hydroperoxides and other  $\text{RO}_2$  to form primarily nitrooxy carbonyls.

## Introduction

Nitrogen oxides ( $\text{NO}_x = \text{NO}_2 + \text{NO}$ ), emitted primarily via lightning or anthropogenic and biogenic combustion processes, play a significant role in the chemistry of the troposphere. In the major daytime radical cycling pathway of  $\text{NO}_x$ ,  $\text{NO}_2$  is photolyzed to  $\text{NO}$  and oxygen atoms, which then react with  $\text{O}_2$  to form ozone ( $\text{O}_3$ ). Reaction of  $\text{NO}$  with  $\text{O}_3$  reforms the  $\text{NO}_2$ . This sets up, during the daytime, a steady-state ratio  $[\text{NO}_2]/[\text{NO}]$  of between 1 and 10 in the boundary layer. Occasionally,  $\text{NO}$  reacts with organic peroxy radicals ( $\text{RO}_2$ ) or hydroperoxy radicals ( $\text{HO}_2$ ) to regenerate  $\text{NO}_2$ . By breaking the  $\text{O}_2$  bond in the  $\text{RO}_2$ , this process results in the net formation of  $\text{O}_3$ , an oxidant and greenhouse gas that is harmful to human health<sup>1,2</sup> (Reactions 1-3).



In addition to these radical propagation cycles,  $\text{NO}_x$  will undergo a series of radical termination reactions, leading to the formation of mono- and multi-functional organic nitrates ( $\text{RONO}_2$ ) or nitroaromatic compounds. While these nitrogen-containing organic compounds can act as sinks of  $\text{NO}_x$ , either by deposition or gas-particle partitioning, they can also undergo transport to locations removed from the original source and re-release  $\text{NO}_x$  via photolysis or further reaction.<sup>1,3</sup> Therefore, quantification of the formation and fate of organic nitrogen chemistry is important for properly modelling  $\text{NO}_x$  chemistry locally, regionally, and globally.

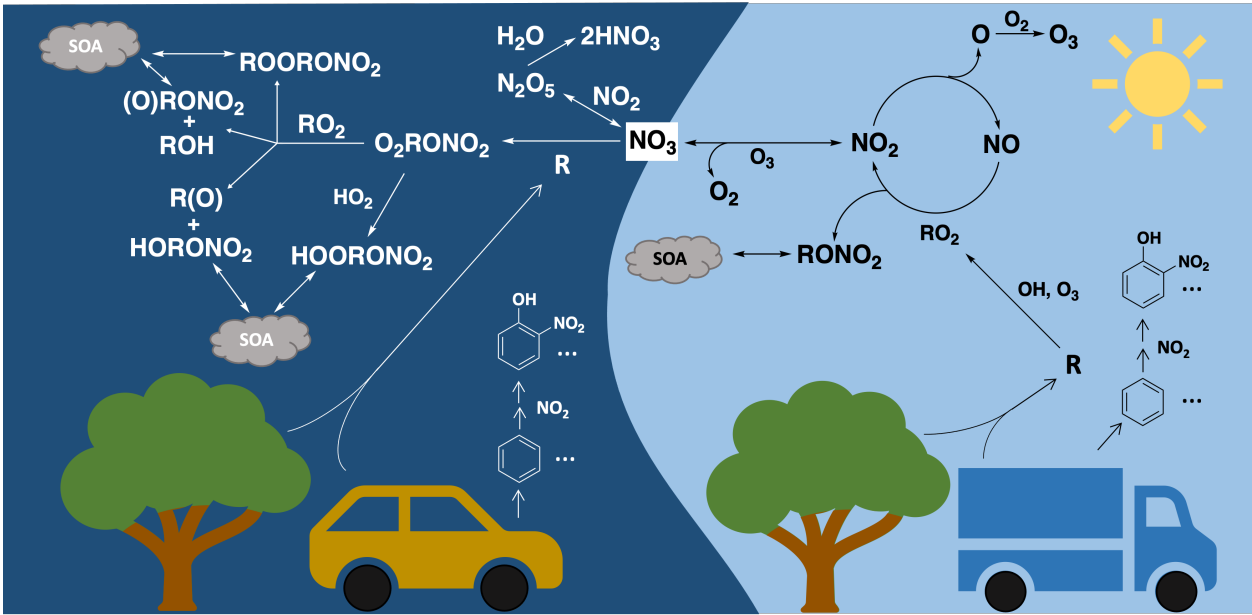
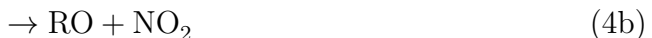


Figure 1: Simplified scheme showing the NO<sub>x</sub> radical cycle and reactions leading to the formation of organic nitrogen during the daytime (right panel) and the nighttime (left panel).

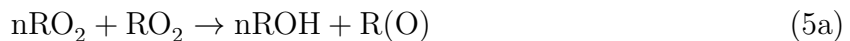
During the daytime, the formation of RONO<sub>2</sub> primarily proceeds by reaction of NO with RO<sub>2</sub> (Figure 1). These RO<sub>2</sub> are typically produced in the OH-initiated oxidation of hydrocarbons, either via OH and subsequent O<sub>2</sub> addition to a double bond (in which case reaction with NO forms  $\beta$ -hydroxy nitrates) or, following hydrogen abstraction and subsequent O<sub>2</sub> addition (in which case reaction with NO forms an alkyl nitrate). The reaction of RO<sub>2</sub> with NO, in addition to forming RONO<sub>2</sub> in minor yield, primarily leads to the formation of an alkoxy radical, RO and NO<sub>2</sub>:



For sufficiently large RO, intramolecular hydrogen-shift chemistry followed by O<sub>2</sub> addition and subsequent reaction with NO can also yield hydroxy nitrates. The measured yields of

$\text{RONO}_2$  from the reaction of  $\text{RO}_2$  with NO range between 0.1-35% and depend largely on the stability of the  $\text{ROONO}^*$  intermediate.<sup>4</sup> In general,  $\text{RONO}_2$  yields increase with carbon number and pressure, and decrease with temperature. Aromatics and highly oxygenated compounds tend to have much lower nitrate yields.<sup>5,6</sup>

In addition to the daytime formation pathway, organic nitrates are formed at night via addition of  $\text{NO}_3$  and, subsequently  $\text{O}_2$ , to alkenes to form a nitrooxy peroxy radical ( $\text{nRO}_2$ ). These  $\text{nRO}_2$  subsequently react with  $\text{HO}_2$  yielding hydroperoxides or with other  $\text{RO}_2$  to produce both carbonyl and hydroxy nitrates, peroxides, or nitrooxy alkoxy radicals:



where  $\text{nROH}$  is a hydroxy nitrate and  $\text{nR(O)}$  is a nitrooxy carbonyl. In many laboratory experiments, including some described here, the  $\text{nRO}_2$  react with  $\text{NO}_3$  yielding, typically, alkoxy radicals which can undergo scission reactions. Although reaction with  $\text{NO}_3$  generally accounts for a smaller fraction of the total atmospheric oxidation of alkenes than reaction with OH, the yield of nitrates is much higher for these reactions (with yields of up to 80%).<sup>7,8</sup> Therefore, under some conditions, these reactions account for up to 50% or more of the total  $\text{RONO}_2$  formed.<sup>4</sup>

The measurement of  $\text{RONO}_2$  has historically been quite difficult, due to the high degree of functionalization and the wide variety of  $\text{RONO}_2$  present in the atmosphere. The development of thermal dissociation laser-induced-fluorescence methods (TD-LIF) to measure total alkyl nitrate concentrations greatly improved the study of ambient nitrate chemistry and the technique has been utilized to measure the (previously underestimated) role of  $\text{RONO}_2$  chemistry in several regions.<sup>4</sup> However, the importance of measuring individual  $\text{RONO}_2$  can-

not be discounted, as  $\text{RONO}_2$  of varying sizes and with varying functional groups will have different atmospheric fates. For example, nitrates that are highly functionalized are more likely to partition to aerosol due to their decreased volatility, while nitrates that retain a double bond are more likely to undergo further oxidation.<sup>4</sup> Additionally, measurements of the relative concentrations of various  $\text{RONO}_2$  can provide significant insight into the local chemistry of a region. For example, while Beaver et al. found that biogenically-derived nitrates accounted for approximately two-thirds of the total alkyl nitrates in a forested region near Sacramento during the 2009 BEARPEX campaign, Teng et al. found that the nitrate chemistry of small alkenes plays a significant role in oxidant formation in Houston.<sup>1,3</sup> On the other hand, at the Bakersfield supersite during the CalNex campaign in 2010, VOC measurements were used to estimate that long-chain alkanes from anthropogenic sources were the largest source of alkyl nitrates during the day, followed by isoprene, aromatics, and alkenes, while monoterpenes dominated nighttime formation of alkyl nitrates with small contributions from isoprene and alkenes.<sup>9</sup> Thus, the prominence of various precursors in nitrate chemistry varies drastically by location and time of day. Speciation of ambient alkyl nitrates can further elucidate the importance of competing formation pathways of nitrate products, such as the formation of nitrooxy-hydroperoxide compounds from  $\text{RO}_2 + \text{HO}_2$  chemistry at night.<sup>10</sup> Therefore, measurements of individual alkyl nitrates and their relative importance in various regions are necessary to better constrain nitrate chemistry and how it differs across various environments.

In addition to the effects of nitrate chemistry on oxidant formation, the formation of low-volatility organic nitrates can lead to the growth of secondary organic aerosol (SOA).<sup>11</sup> Previous ambient measurements have demonstrated that the organic nitrates formed in the gas-phase are significant components of organic aerosol mass, with molecules containing organonitrate groups estimated to contribute up to 10% of total organic mass in submicron particles in some regions.<sup>12,13</sup> The contribution of nitrates to aerosol loading appears to be especially important during the night, where  $\text{NO}_3$ -derived organic nitrates have been mea-

sured to constitute as much as one-third of nighttime increases in organic aerosol.<sup>13–15</sup> A strong connection between the concentrations of VOC precursors and corresponding particulate organic nitrate has been observed, further demonstrating that the organic nitrates formed in the gas-phase processes discussed above are likely to partition into the particle phase.<sup>14</sup> However, the contribution of organic nitrates throughout the diurnal period has not been measured in a variety of regions, and the effect of NO<sub>x</sub> reductions in major cities due to emissions regulations is not well understood.

In this work, we aim to create a census of the important functionalized organic nitrogen-containing compounds present in the Los Angeles urban atmosphere during the 2021 RECAP-CA campaign. We examine the composition of these compounds in both the gaseous and particle phase and, by comparison to laboratory data, identify several of the compounds observed in the ambient gas-phase atmosphere. We then examine the roles played by biogenic hydrocarbons, alkenes, and aromatic compounds in the nitrogen budget of the urban atmosphere in this region.

## Methods

### Sampling Period and Location

The Re-Evaluating the Chemistry of Air Pollutants in California (RECAP-CA) campaign took place between June and August 2021 on the Caltech campus in Pasadena, California (34.14°N, -118.13°W). The suburban location is approximately 18 km northeast of downtown Los Angeles and 7 km south of the San Gabriel mountain range, with prevailing winds during the day coming from the south. Anthropogenic NO<sub>x</sub> emissions from downtown Los Angeles heavily influence the chemistry at this site, with an average daytime NO value of 1.7 ppb and an average NO<sub>2</sub> to NO ratio ratio of 7.7 measured during the time period examined here (Figure 2). Additionally, biogenic VOC emissions play a significant role in the chemistry, with local vegetation emitting copious amounts of isoprene and monoterpenes, especially at

high ambient temperatures. We therefore expect both NO<sub>x</sub> chemistry and isoprene chemistry to be prominent at the site.

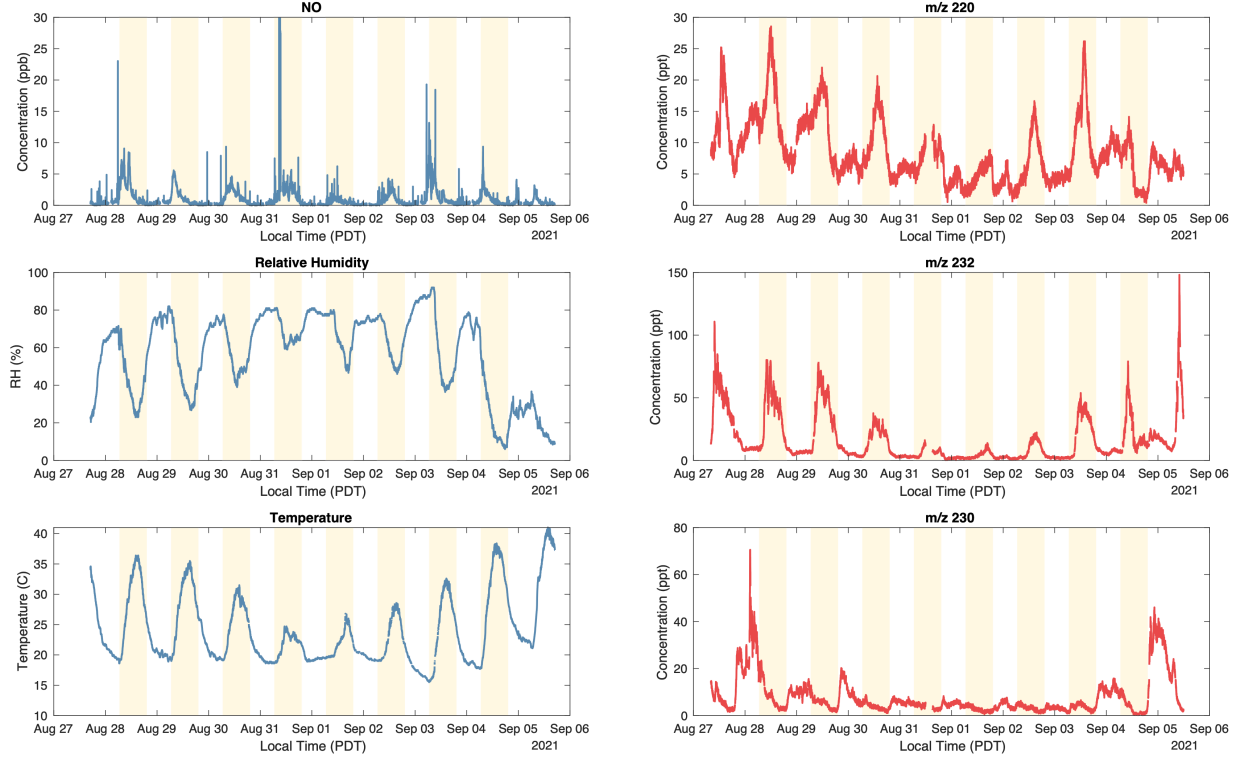


Figure 2: Daily conditions at the sampling site between August 28th, 2021 and September 5th, 2021 compared to concentrations of representative compounds measured with the Caltech CToF-CIMS. NO concentration (ppb, upper left panel) and temperature (°C, lower left panel) measurements were conducted at the California Institute of Technology Air Quality Station (CITAQS). NO concentrations were measured in the CITAQS with a Teledyne T200U. Note that, on August 31st at approximately 8:45 AM PDT, there NO concentration spiked to a value of approximately 220 ppb. This spike was due to a truck idling beside the sampling area. Relative humidity (RH, %, middle left panel) was measured by the TCCON weather station on top of the Linde Laboratory using a Vaisala HMP60 temperature and humidity probe. Concentrations, in ppt, of compounds present at m/z 220 (e.g. C4 hydroxy nitrates, upper right panel), m/z 232 (e.g. isoprene-derived hydroxy nitrates, middle right panel), and m/z 230 (e.g. isoprene-derived nitrooxy carbonyls, lower right panel) as measured by the CToF-CIMS are shown for comparison. Structures corresponding to compounds observed at m/z 220 are given in Table 3, structures corresponding to compounds observed at m/z 232 are given in Table 1, and structures corresponding to compounds observed at m/z 230 are shown in Table 2. Yellow shaded rectangles show the periods between sunrise and sunset on each day.

The Caltech gas chromatograph chemical ionization high resolution time-of-flight mass spectrometer (GC-HRToF-CIMS) and compact time-of-flight mass spectrometer (CToF-MS), which are described later, were both deployed on the second floor of the Ronald and Maxine Linde Laboratory for Global Environmental Science on the southwest corner of the campus. Both instruments were housed inside an unused office space with a common Teflon inlet, approximately 2m long, sampling outside of the window, at a height of approximately 7 m above the ground. Very high flows were maintained through this inlet such that the residence time was less than 0.2s. The CToF sampled from the inlet between August 4th, 2021 and September 5th, 2021, while the GC-CIMS sampled between August 9th, 2021 and September 7th, 2021. In this study, we focus on the time period between August 28th, 2021 and September 5th, 2021, as this period encompassed the overlap of both high quality GC-CIMS data and high quality CToF data. The average daily maximum temperature during this time period was 33.2°C, with an average daily minimum temperature of 18.6°C. The relative humidity (RH) was 57% on average, with an average daily maximum RH of 76% at night and a minimum daily average RH of 30% typically reached in the mid afternoon (Figure 2).

## Instrumentation

### GC-HRToF-CIMS

The Caltech GC-HRToF-CIMS has been described in detail elsewhere,<sup>16</sup> but a brief description and the details of operation during the campaign are given here.

The HRToF-CIMS uses  $\text{CF}_3\text{O}^-$  as a reagent ion, a soft ionization method that is particularly sensitive to multifunctional organic compounds.<sup>17</sup> The reagent ion is produced by passing  $\text{CF}_3\text{OOCF}_3$  gas, diluted with  $\text{N}_2$ , through a tube coated with polonium-210 (NRD, Po-2021). Although the GC-CIMS can be operated in direct sampling mode such that gas is sampled directly into the HRToF, during the time period discussed here the HRToF-CIMS exclusively sampled the effluent of the GC. The metal-free GC consists of a 2 m fused silica

column (Restek RTX-1701) that is cooled with the expansion of liquid CO<sub>2</sub> and heated with resistance heaters controlled with a Watlow temperature controller. Approximately 4000 sccm of ambient air was sampled from the main inlet via a 1 inch O.D.(?) Teflon tube and directed towards the GC. The GC sub-sampled approximately 1200 sccm [140??] from this flow every hour for either 2 or 15 minutes. The flow was then diluted with 1440 sccm of N<sub>2</sub>, diluting the sample by a factor of 10. Analytes were trapped on a small length of column [how long] at -10°C prior to the 2 m GC column. When trapping was complete, the temperature of the GC and the trap was increased from -10°C to 20°C at 13°C/min, from 20°C to 50°C at 3°C/min, and from 50°C to 130°C at 10°C/min. A flow of 5 sccm of N<sub>2</sub> flowed through the column during this elution period. Immediately after the oven, the column effluent was combined with 200 sccm N<sub>2</sub> to rapidly transport the column effluent to the ion source, where it combined with an additional 180 sccm N<sub>2</sub> containing ppm levels of CF<sub>3</sub>OOCF<sub>3</sub>. To maximize the signal-to-noise ratio, the column output was flowed directly through the ion source, intersecting with 1500 sccm N<sub>2</sub> from the Teflon-coated pyrex flow tube. Here, analytes react with CF<sub>3</sub>O<sup>-</sup> to form cluster or fluoride transfer product ions. The ionized analytes are then directed into the mass spectrometer by a conical hexapole ion guide, where they are subsequently detected at a mass-to-charge ratio of their molecular weight plus the mass of CF<sub>3</sub>O<sup>-</sup> ( $m/z = mw + 85$ ) or their molecular weight plus the mass of fluorine ( $m/z = mw + 19$ ). After reaching 130°C, the column temperature was held constant for two minutes before cooling to -10°C to repeat the sampling. This procedure was fully automated and for the time period analyzed here samples were taken throughout the day and night, with occasional short pauses for maintenance procedures or data reduction.

## CToF-CIMS

The CToF-CIMS uses an ionization scheme identical to that described above. The instrument was essentially unchanged from the configuration described by Allen et al.<sup>18,19</sup> and Xu et al.<sup>20</sup> except that the external aircraft inlet was replaced by the 2 m Teflon tube discussed

above. A centrifugal blower was used to maintain a large flow, and thus a short residence time (<0.2s) in the ambient pressure inlet. The CToF does not have chromatography and the mass resolution of the mass filter is approximately four times lower than the GC-HRToF.

## Aerosol Mass Spectrometer

Ambient submicron, non-refractory particulate matter (NR-PM1) was measured during the campaign using an Aerodyne High Resolution Time-of-Flight Aerosol Mass Spectrometer (HR-ToF-AMS; hereafter “AMS”). The AMS was housed on the second floor of Linde Laboratory and sampled ambient air through approximately 8 m of 3/8” OD stainless steel line connected to a 2.5  $\mu\text{m}$  Teflon-coated cyclone mounted on the roof. No direct drying of the sample stream was performed, but in-line measurements confirmed that the humidity of the sampling line did not exceed 50%. Data were measured using the “V-mode” ion flight path through the time-of-flight chamber and analyzed using the SQUIRREL v1.65C and PIKA v1.25C software packages. Standard methods were used to correct the data for gas-phase interferences and composition-dependent collection efficiencies.<sup>21</sup> Elemental analysis of organic aerosol composition was performed using the “Improved-Ambient” method.<sup>22</sup> The ionization efficiency (IE) of nitrate and relative ionization efficiencies of ammonium and sulfate were calibrated using dry, 350-400 nm ammonium nitrate and ammonium sulfate particles approximately every week during each campaign. Concentrations of organic (NO<sub>3,org.</sub>) and inorganic (NO<sub>3,inorg.</sub>) nitrates measured by the AMS were estimated using the NO<sub>x</sub> ratio method. Briefly, laboratory measurements have demonstrated that nitrate functionalities associated with organic and inorganic nitrates fragment to produce considerably different NO<sup>+</sup>/NO<sub>2</sub><sup>+</sup> ion ratios in the AMS, termed R<sub>ON</sub> and R<sub>AN</sub>, respectively.<sup>23</sup> While the specific R<sub>ON</sub> and R<sub>AN</sub> values vary between instruments, we used the procedure of Fry et al.<sup>13</sup> and assumed that the R<sub>ON</sub>/R<sub>AN</sub> value is instrument independent. R<sub>AN</sub> values were calculated from IE calibration data using pure ammonium nitrate particles. We used an R<sub>ON</sub>/R<sub>AN</sub> value of 3.99  $\pm$  0.25 following Xu et al.,<sup>24</sup> which represents values observed for  $\beta$ -pinene

organic nitrates in laboratory studies.

## Instrument Calibration

The sensitivity of the CToF-CIMS to several compounds discussed here, including isoprene hydroxy nitrate, has been measured previously in our laboratory using pure synthetic standards.<sup>25,26</sup> The relative sensitivities of the CToF-CIMS to other compounds, including isoprene nitrooxy-carbonyl and isoprene nitrooxy hydroperoxide, have been estimated using theoretical calculations of the relative rates of ion-molecule collisions.<sup>27,28</sup> Due to the wide range of compounds studied here, the lack of authentic standards for most of these compounds, and the difficulty of synthesizing authentic standards, the sensitivity of the GC-HRToF-CIMS to the compounds analyzed in this work were scaled from the observations made using the CToF-CIMS. To determine a multiplicative factor for the relationship between the sensitivities of the two instruments, we compared the average diurnal signal of m/z 232 (the signal dominated by isoprene hydroxy nitrates) in the CToF-CIMS and the GC-HRToF, and found that the CToF-CIMS was approximately 1.4 times more sensitive to these compounds than the GC-HRToF-CIMS. This ratio was then used to estimate the sensitivity of the GC-HRToF-CIMS by comparison to the CToF-CIMS sensitivity (either calculated or measured, where available) for all of the compounds discussed in this work. A table of these sensitivities is included in the SI.

Using  $\text{CF}_3\text{O}^-$  as a reagent ion, organic compounds containing a single nitrogen atom are observed at even m/z. Some signal from the <sup>13</sup>C and <sup>17</sup>O isotopologues of non-nitrogen containing compounds also contribute to this signal. In the following analysis, these contributions are estimated using the signal at m/z-1 and an estimate of the isotope ratio based on the mass, and subsequently subtracted from the signal at the even m/z.

## Laboratory Experiments

Laboratory oxidation experiments were performed to assign the elution temperatures for several organic nitrates expected to be observed in the ambient data. Two experiment types, ‘light’ and ‘dark’ oxidation experiments, were performed for several precursor alkenes. The general procedures for both of these experiments are described below.

In the ‘light’ oxidation experiments, oxidation of precursor alkenes by OH was initiated via the photolysis of H<sub>2</sub>O<sub>2</sub> at 254 nm. In a typical experiment, 1000 ppb of H<sub>2</sub>O<sub>2</sub>, between 50 and 500 ppb of the precursor alkene, and 1000 ppb of NO were injected into the 800-liter FEP Teflon environmental chamber. Under these conditions, OH addition followed by O<sub>2</sub> addition to the precursor alkenes leads to formation of a suite of peroxy radicals, which react with NO to form hydroxy nitrates (Reaction 4a). To create these conditions, H<sub>2</sub>O<sub>2</sub> (30% by weight, Macron Fine Chemicals) was injected into the chamber by weighing the desired amount into a pre-weighed, three-way glass vial and flowing air through the vial and into the chamber at a rate of 20 SLM. To ensure that the evaporation of the sample was complete, the vial was reweighed after the injection. NO was measured into a 500 mL glass bulb using manometry, with the bulb attached in series with a vacuum/N<sub>2</sub> dilution system and a tank of 1993 ppm NO (Matheson). The desired concentration, typically 1000 ppb, was then reached by serial dilution, with pressure measurements conducted by MKS 1000 and 10 Torr baratron pressure transducers. The purity of the NO sample was confirmed by obtaining an IR spectrum of the resulting bulb contents in a 19 cm pyrex FTIR cell with CaF<sub>2</sub> windows. The NO was then injected (prior to initiation of photolysis) by flowing dry air at 20 SLM through the bulb until the contents of bulb were flushed into the environmental chamber.

Eight Sankyo Denki 254 nm lamps were energized for 1-5 minutes to photolyze the H<sub>2</sub>O<sub>2</sub> and initiate the alkene oxidation. In many of the experiments, multiple precursor alkenes were oxidized simultaneously for efficiency. The details of individual experiments are given in the SI — the ‘light’ oxidation experiments were performed with propene ( $\geq 99\%$ , Sigma Aldrich), ethene ( $\geq 99.5\%$ , Sigma-Aldrich), isoprene (99%, Sigma Aldrich), 1-butene ( $\geq$

99%, Sigma Aldrich), 2-methylpropene (99%, Sigma Aldrich), 1-pentene ( $\geq$  98.5%, Sigma-Aldrich), pentane (98%, Sigma-Aldrich), and hexane ( $\geq$  99%, Sigma-Aldrich). With the exception of trapping time and sample dilution, which were altered due to the significantly higher abundance of nitrates and lower water concentrations under the laboratory conditions, all gas chromatograms in these experiments were performed under the same conditions as those performed in the field.

In the ‘dark’ oxidation experiments,  $\text{NO}_3$  was formed via the reaction of  $\text{NO}_2$  and  $\text{O}_3$  (Reactions 6-7).



In a typical experiment, the chamber was first filled with 40 liters of dry air. Following this, between 50-100 ppb of  $\text{O}_3$  was injected using an  $\text{O}_3$  generator (Enmet, Model 04051-011) flowing at 1.5 SLM. Simultaneously, the  $\text{O}_3$  concentration was monitored using a Teledyne 400E Photometric  $\text{O}_3$  Analyzer sampling at 1.5 SLM, thus ensuring that the total volume of air in the chamber did not change during this injection step. The ozone generator was turned off when the desired concentration was reached. With the  $\text{O}_3$  instrument still sampling, a further 160 liters of dry air was injected into the chamber at 20 SLM. Once the ozone concentration in the chamber was stabilized following this dilution step, direct sampling from the CIMS instrument was initiated and  $\text{NO}_2$  was injected into the chamber, leading to the immediate formation of  $\text{N}_2\text{O}_5$  and  $\text{NO}_3$ .  $\text{NO}_2$  was measured into a 500 mL glass bulb in the same manner described for  $\text{NO}$ , and injected by flushing the bulb with dry air at 20 SLM into the environmental chamber. Following the injection of  $\text{NO}_2$ , a background GC was taken of the chamber contents, using the same GC conditions as described for the ‘light’ oxidation experiments (once again, a description of the exact conditions used in each experiment is given in the SI). Upon completion of this GC, direct sampling was initiated

and approximately 50-500 ppb of the precursor alkenes were injected. The alkenes were measured into a 500 mL glass bulb in the same manner described for NO and NO<sub>2</sub>, and injected by flushing the bulb with dry air into the environmental chamber at 20 SLM. Oxidation began immediately upon injection of the precursor alkenes—‘dark’ oxidation studies were performed with 2-methylpropene (99%, Sigma Aldrich), cis-2-butene ( $\geq$  99%, Sigma Aldrich), propene ( $\geq$  99%, Sigma Aldrich), 2-methyl-2-butene ( $\geq$  99%, Sigma Aldrich), isoprene (99%, Sigma Aldrich), 2-methyl-1-butene (analytical standard, Fluka), 1,3-butadiene ( $\geq$  99%, Sigma Aldrich),  $\alpha$ -pinene ( $\geq$  99%, Sigma Aldrich), 2-methyl-2-pentene (> 98%, Fluka), cis-2-pentene (98%, Sigma Aldrich), 1-butene ( $\geq$  99%, Sigma Aldrich), and furan ( $\geq$  99%, Sigma Aldrich). Two minutes after the alkene injection, a GC of the system was taken. A second GC was taken approximately 50 min after the first, once the reaction had progressed further. Due to the complexity of the products in these experiments, hydrocarbons were generally injected individually rather than in groups, as was sometimes done in the case of the ‘light’ oxidation experiments. In these experiments, the nitrooxyperoxy radicals react with both NO<sub>3</sub> and HO<sub>2</sub>, with the latter formed via the decomposition of the organic alkoxy radicals. Consistent with formation of significant amounts of HO<sub>2</sub>, formation of hydroperoxynitrate, HO<sub>2</sub>NO<sub>2</sub>, is observed in these experiments.

## Results and Discussion

### Diurnal Profiles

The average diurnal profiles of the concentrations of organic nitrates at several representative even m/z, measured with both the GC-CIMS and the CToF, are shown in Figure 3. These diurnal profiles match quite closely across both instruments throughout the observation period. For compounds at lower mass-to-charge ratios, such as m/z 206 (hydroxynitrates from the oxidation of propene), the measured GC concentrations tend to be lower than those measured by the CToF. This observation is consistent with inefficient trapping of the more

volatile nitrates at the relatively high trapping temperatures used during the campaign. For example, in the laboratory, we find that the trapping efficiency of propene-derived hydroxy nitrates ( $m/z$  206) is approximately 45% under the conditions used during the campaign, consistent with the difference in the average measured GC and CToF concentrations at  $m/z$  206 in the ambient data (Figure 3a).

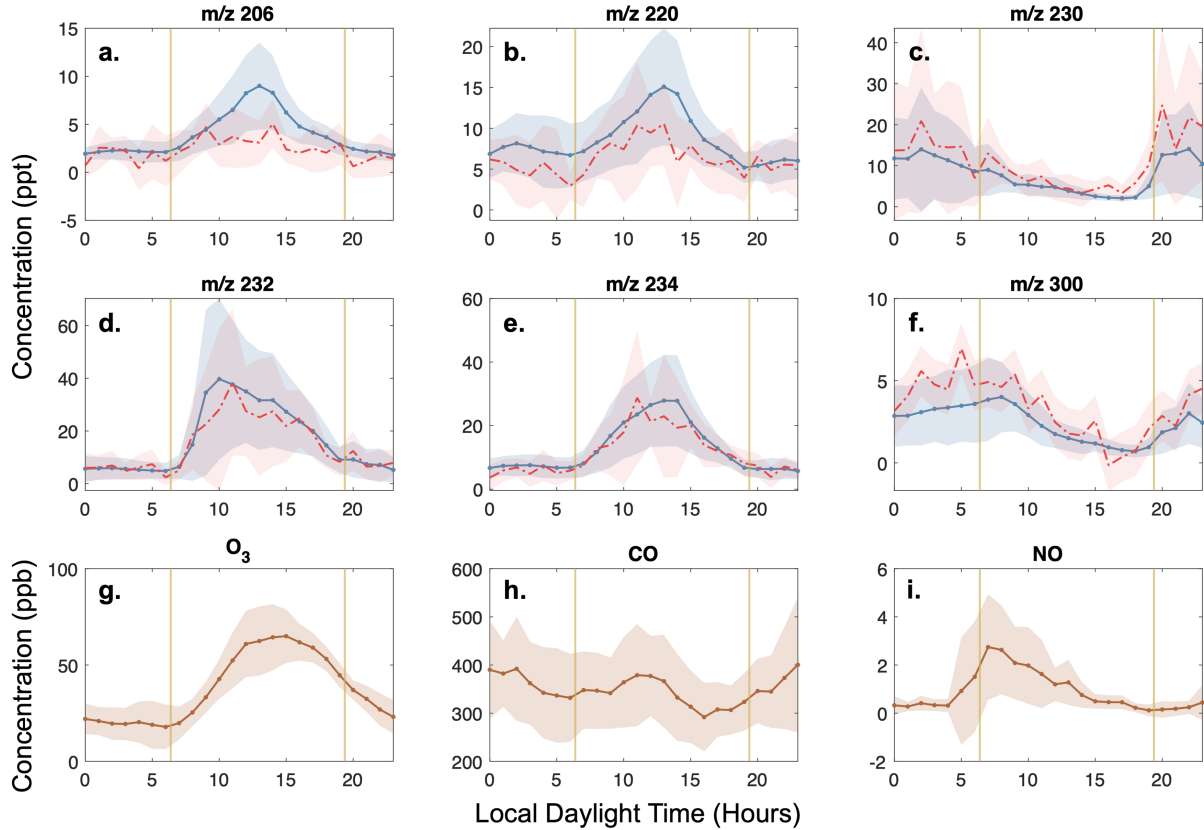


Figure 3: Average diurnal profiles of representative masses from August 28th – September 5th. The top two panels (a–f) show the average diurnal profiles (in pptv) of representative masses from August 28th – September 5th, measured with both the GC-CIMS (in red) and the CToF (in blue).  $m/z$  206 (a) corresponds to the mass of propene-derived hydroxy nitrates,  $m/z$  220 (b) are C4-derived hydroxy nitrates,  $m/z$  230 (c) is the mass of isoprene-derived nitrooxy carbonyls,  $m/z$  232 (d) are the isoprene-derived hydroxy nitrates,  $m/z$  234 (e) includes C5 hydroxy nitrates and MVK/MACR-derived nitrates, and  $m/z$  300 (f) includes monoterpene-derived hydroxy nitrates. The shaded area encompasses  $1\sigma$  over the time period. Yellow vertical lines denote the local sunset and sunrise times. The lower panel (g–i) gives the average diurnal profiles (in ppbv) of  $O_3$ , CO, and NO as measured by the CIT-AQS during the same time period, with the shaded area showing  $1\sigma$ .

The diurnal profiles seen in Figure 3 generally fall into two categories: signals composed primarily of nitrogen-containing organic compounds formed during the daytime (NCOC-day) and nitrogen-containing organic compounds formed during the nighttime (NCOC-night). In general, NCOC-day increase at sunrise (between 5 and 8 AM local time), with a peak in the afternoon, followed by a steady decrease throughout the late afternoon and evening until reaching nighttime concentrations that are typically less than 1/3 of those observed during the daytime. As the sun sets at approximately 6 PM, there is a sudden increase in NCOC-night followed by a steady increase throughout the evening and a steady decrease during the daytime. At some m/z (such as m/z 248), both NCOC-day and NCOC-night contribute significantly to the overall signal, leading to more complicated diurnal profiles. The approximate times of sunset and sunrise during the time of the campaign are shown as vertical lines on the figures. For the majority of this analysis, ‘daytime’ refers to the time period between 8:00 AM and 8:00 PM, whereas ‘nighttime’ refers to the time period between 8:00 PM and 8:00 AM—where different definitions are used, the difference is noted.

The chromatographic data show that the NCOC-day and NCOC-night shown in Figure 3 are composed of a large number of compounds that contribute to the signal at a given mass-to-charge ratio. In the next sections, we identify some of the individual compounds that contribute to NCOC-day and NCOC-night and touch upon the implications for urban organic nitrate chemistry.

## Biogenic Nitrates

As is evident in Figure 4, organic nitrogen compounds derived from the oxidation of biogenic hydrocarbons (including isoprene-derived and monoterpene-derived NCOC) contribute a significant fraction of the total concentration of gas-phase organic nitrates observed during the time period discussed here. The total contribution of the sum of isoprene- and terpene-derived organic nitrates peaked during the morning at an average of 35% of the total signal observed over all even m/z. This contribution increased to approximately 37% of the total

signal at even m/z on days with maximum temperatures greater than 30°C. Of the gas-phase biogenic nitrates identified here, the nitrates of isoprene contributed most significantly to the total organic nitrate concentration, carrying 33% of the total signal observed at even m/z during this time period. The prominence of biogenic emissions in observed gas-phase organic nitrogen formation is generally consistent with analyses of emissions in June of 2021, which found that up to 60% of total VOC OH reactivity, ozone formation potential, and SOA formation potential could be attributed to emissions of biogenic terpenoid compounds and that this contribution is most significant at high temperatures.<sup>29</sup> However, although in both studies biogenic compounds are observed to be prominent, the estimated contribution of these biogenic compounds appears to be higher in the analysis of Pfannerstill et al. than the contribution to the overall organic nitrogen budget observed in this study. This is likely due in part to the rapid hydrolysis of isoprene-derived hydroxy nitrates,<sup>30</sup> which likely leads to an underestimate of the total isoprene hydroxy nitrates formed in the gas-phase.

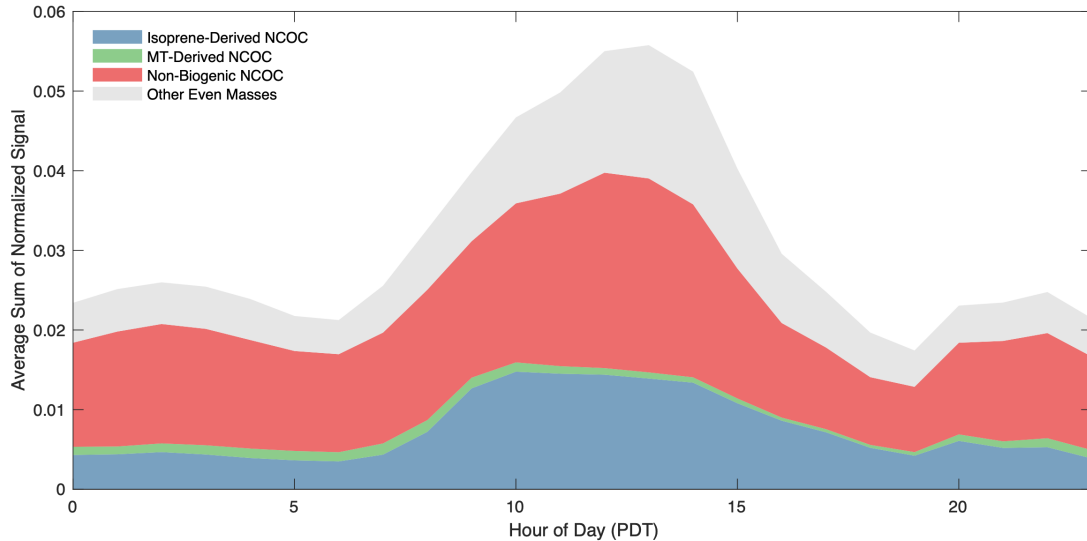


Figure 4: The average total signal observed by the CToF-CIMS at isoprene-derived nitrate masses ( $m/z$  232, 40% of  $m/z$  230,  $m/z$  248, and 49% of  $m/z$  234) in blue, monoterpene (MT)-derived nitrate masses ( $m/z$  = 298, 300, and 316) in green, and other non-biogenic nitrates ( $m/z$  = 158, 172, 190, 192, 204, 206, 218, 220, 60% of 230, 51% of 234, 236, 246, 250, and 264) in red, as a function of hour of day over the time period examined here. The average sum of the signal at other even masses is given in grey. The signals at  $m/z$  230 and  $m/z$  234 are split across categories as they contain multiple organic nitrate products with different sources. These breakdowns are discussed further in the main text and in the SI.

### Hydroxy Nitrates of Isoprene (IHN)

Isoprene-derived hydroxy nitrates (mw 147) are observed at  $m/z$  232 in our  $\text{CF}_3\text{O}^-$  CIMS. The diurnal profile of the signal at  $m/z$  232 (Figure 3d) is consistent with products primarily formed during the daytime, with the average concentration reaching a peak of approximately 40 ppt at 10 AM. The lower panel of Figure 5 shows a sum of the ambient chromatograms taken on 08/28/2021 during both the daytime and the nighttime, with the nighttime ambient data multiplied by a factor of three for clarity. These traces are largely representative of the ambient chromatographic data at  $m/z$  232 observed throughout RECAP. The daytime signal is dominated by two compounds, eluting at  $73.1^\circ\text{C}$  and  $77.8^\circ\text{C}$ , while at night the signal is carried by a variety of other compounds.

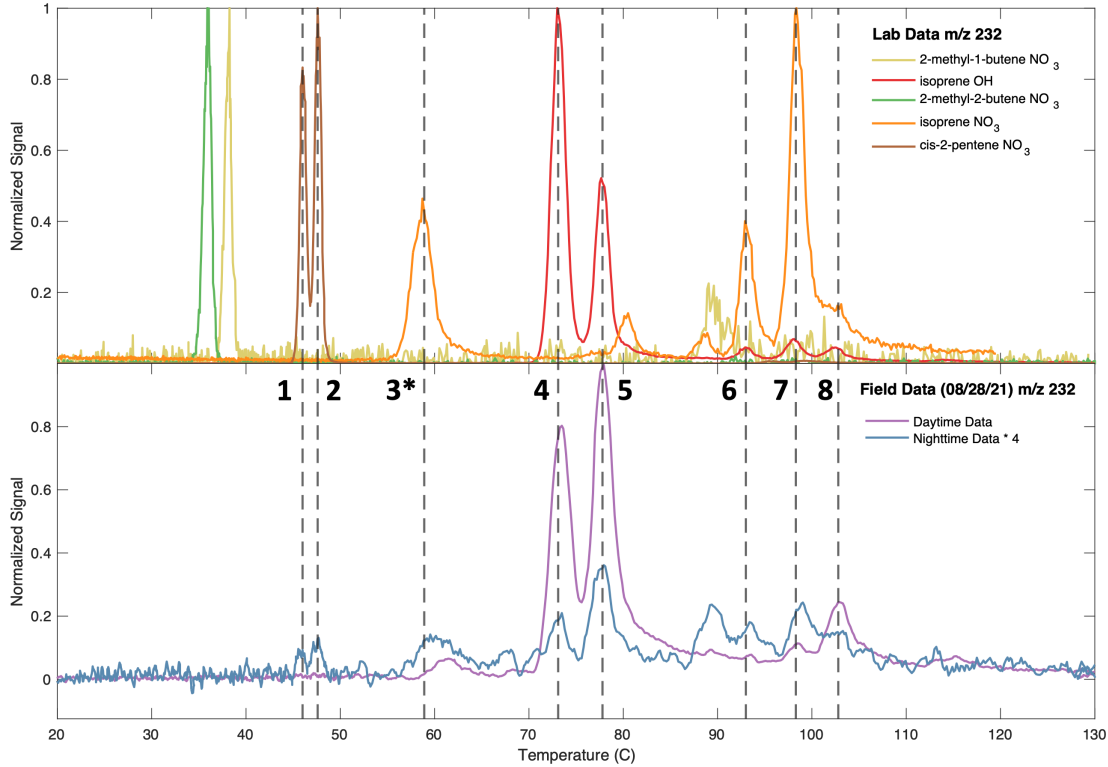


Figure 5: Ambient chromatographic data (lower panel) from 08/28/2021 with daytime signal in purple and nighttime data in blue. The nighttime signal is multiplied by a factor of 4 for clarity. Each trace in the lower panel is a sum of the traces during the daytime and nighttime period. Chromatographic data from a series of laboratory oxidation experiments (upper panel) are shown for comparison. Vertical dashed lines are drawn to align peaks in the laboratory and field data. The small shoulder of peak 3 eluting at  $\sim 59^{\circ}\text{C}$  in the laboratory oxidation of isoprene has been tentatively assigned to the hydroxynitrate formed via OH addition at C3.<sup>31</sup>

While isoprene-derived hydroxy nitrates constitute the majority of the signal at  $\text{m/z}$  232, other compounds (such as nitrooxy carbonyls derived from C5 alkenes) also appear at this mass. To confirm the identity of the observed compounds, elution temperatures were compared to those of the products observed in the dark and light oxidation experiments of 2-methyl-1-butene, isoprene, 2-methyl-2-butene, and cis-2-pentene. A list of assignments for the peaks shown in Figure 5, where assignments were possible, is given in Table 1. The cis-2-pentene-derived nitrooxy carbonyls that are assigned to peaks 1 and 2 are discussed in the section on anthropogenic nitrates.

Table 1: Assignments of chromatographic peaks observed in ambient data at m/z 232. Peak numbers correspond to the peak numbers given in Figure 5. A star indicates that the peak appears to encompass two or more compounds.

Peak	Elution Temperature (°C)	Assignment
1	46	
2	47.6	
3*	58.9	
4	73.1	
5	77.8	
6	93	
7	98.3	
8	102.8	

The two major daytime peaks at this mass (peaks 4 and 5), which are identified using the assignments from Teng et al.,<sup>31</sup> correspond to two  $\beta$  isomers (1-OH, 2-N and 4-OH, 3-N) of the isoprene-derived hydroxy nitrates (Table 1). During daytime, these nitrates are significantly more abundant than those of the  $\delta$ -isomers, identified as peaks 6, 7, and 8. This is consistent with the observation that in the atmospheric OH-initiated oxidation of isoprene, the  $\beta$ -isomers constitute approximately 95% of the total isoprene-derived hydroxy peroxy radicals.<sup>31</sup> The relative concentrations of these  $\beta$  isomers, however, are perturbed from the distribution observed in the laboratory. This is due, primarily, to the rapid hydrolysis of the 1-OH, 2-N isomer previously described by Vasquez et al.<sup>30</sup> Consistent with Vasquez et al., the ratio of 1-OH, 2-N to 4-OH, 3-N depends both on time of day (highest mid-day) and

relative humidity (highest on dry days) (Figure S6).

The nighttime signal at m/z 232 includes significant contributions from both  $\beta$ - and  $\delta$ -IHN (isoprene hydroxynitrate). This is in keeping with previous observations that, in the  $\text{NO}_3^-$ -initiated oxidation of isoprene under atmospheric conditions, the concentrations of  $\beta$ -nitrooxy and  $\delta$ -nitrooxy peroxy radicals are approximately equal.<sup>10</sup> The nitrooxy delta peroxy radicals are also much less likely to undergo autoxidation than their OH counterparts.<sup>32</sup> Consistent with the  $\text{NO}_3^-$ -initiated oxidation of isoprene in the laboratory, the formation of the  $\delta$ -isomers (peaks 6, 7, and 8) and the 3-OH, 4N  $\beta$  isomer (peak 3\*) of the hydroxy-peroxy radical are favored. (Figure 5). While there is a small contribution to the overall nighttime signal at m/z 232 from the nitrooxy carbonyl formed in the oxidation of cis-2-pentene (peaks 1 and 2), throughout the daytime and nighttime the signal is (as expected) dominated by the products of  $\text{NO}_3^-$  and, especially, OH-initiated isoprene oxidation.

Following the oxidation of isoprene, additional C4 hydroxy carbonyl nitrates are formed in the oxidation of the major isoprene oxidation products: methyl vinyl ketone (MVK), and the first generation IHN.<sup>32</sup> The nitrates derived from these compounds are observed in our CIMS at m/z 234 and are discussed further alongside the alkene-derived hydroxy nitrates observed at this mass in the section discussing anthropogenic NCOCs.

### Hydroxy Nitrates of Monoterpenes

Nitrates formed in the oxidation of monoterpenes are observed with  $\text{CF}_3\text{O}^-$  CIMS at m/z 300 and 316 (hydroxy and hydroperoxy nitrates, respectively). The diurnal profile of the signal at m/z 300 is consistent with compounds primarily formed in the evening (Figure 3), with an average maximum concentration of approximately 5 ppt before sunrise. Due to their high mass (and resulting poor separation) and the diversity of monoterpenes present in the Los Angeles atmosphere,<sup>33</sup> we are unable to determine the individual molecular contributions to this signal. However, it is clear from Figure 3 that, given the high reactivity of many of the monoterpenes,<sup>34</sup> they represent a significant sink of  $\text{NO}_3^-$  in the nighttime Los Angeles

atmosphere.

### Nitrooxy Carbonyls

Isoprene-derived nitrooxy carbonyls (mw 145) are observed in the CIMS at m/z 230. The diurnal profile of m/z 230 (Figure 3) is consistent with compounds primarily produced during the nighttime, supporting the hypothesis that the signal at this mass originates from the NO<sub>3</sub>-initiated oxidation of isoprene. Consistent with this expectation, four isomers of the nitrooxy carbonyl produced in the laboratory NO<sub>3</sub>-initiated oxidation of isoprene, with identities assigned based on the work of Schwantes et al.<sup>10</sup> (Table 2), match the elution temperatures of compounds observed in the ambient data. However, in the ambient signal we observe a prominent fifth peak—at times carrying more than half of the m/z 230 signal—that is not produced in the NO<sub>3</sub>-initiated oxidation of isoprene in the laboratory (Figure 6).

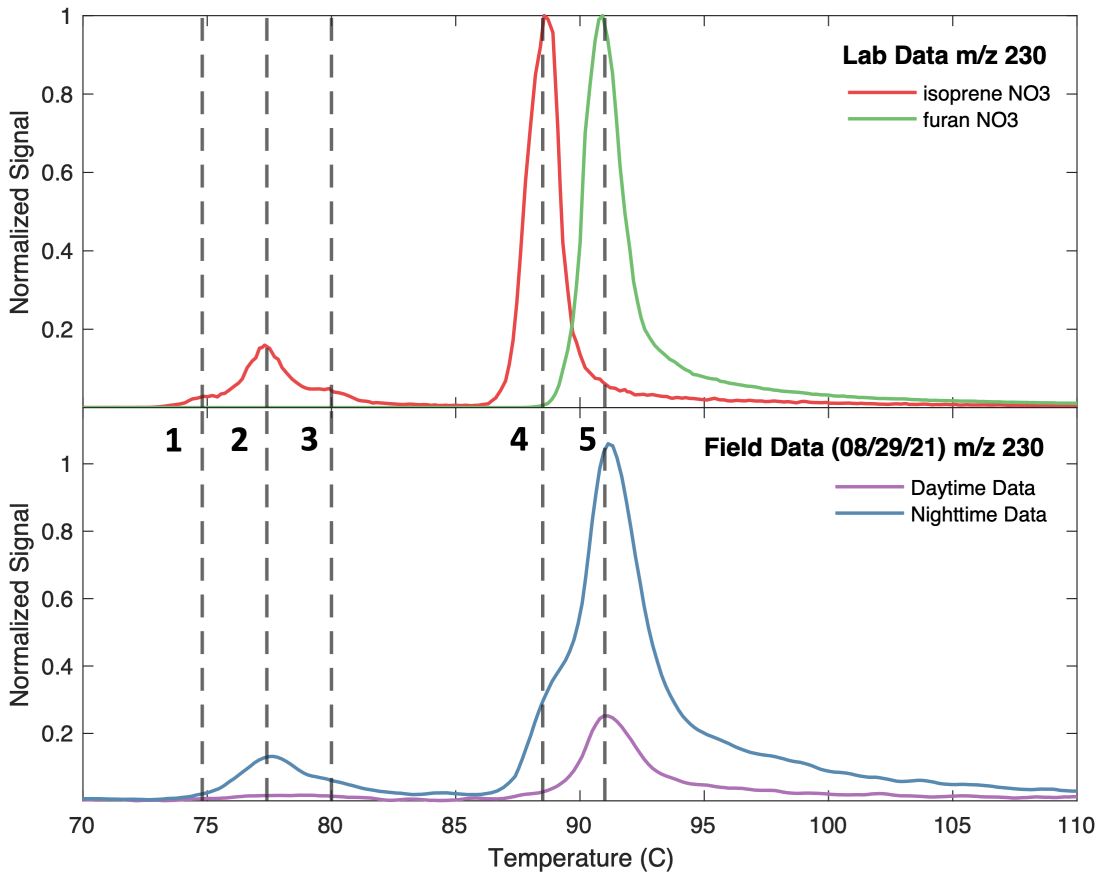


Figure 6: Sum of ambient chromatograms at  $m/z$  230 taken during the daytime and nighttime (lower panel, purple and blue trace, respectively) on 08/29/2021. Chromatographic data at  $m/z$  230 collected during the laboratory oxidations of furan and isoprene by  $\text{NO}_3$  are shown in the upper panel for comparison. Vertical dashed lines are included to show alignments between peaks in the ambient and laboratory data.

This fifth peak persists throughout the daytime, while all four of the peaks corresponding to isoprene nitrooxy carbonyls are only present in significant concentrations at night, consistent with the high OH reactivity of these compounds. The mass of the unique compound is shifted by -.04 amu from the isoprene-derived nitrates. We identify the fifth peak as an organic nitrate compound produced in the  $\text{NO}_3$ -initiated oxidation of furan (Figure 6). Additionally, in deuterium exchange experiments we observe no mass shift (Figure S1), demonstrating that the compound contains no -OH or -OOH functional group. We therefore assign this peak to one of (or a sum of) the carbonyl structures shown in Table 2. While it

is impossible from this data alone to attribute a source to this compound, possible sources include the atmospheric  $\text{NO}_3$ -initiated oxidation of furan (as was observed in the laboratory) or the  $\text{NO}_3$ -initiated oxidation of butadiene. The exact mechanism of the formation of furan in the oxidation of butadiene is unclear, but has been observed in previous work.<sup>35</sup> Both furan and butadiene were observed in the Los Angeles atmosphere during the summers of 2020 and 2022 in concentrations of approximately 10–20 ppt.<sup>33</sup> Considering the relative rates of the reactions of these compounds with  $\text{NO}_3$  (the rate of the reaction of  $\text{NO}_3$  with furan is an order of magnitude faster than that of butadiene), the low yields of furan observed in the reaction of butadiene, and the prominence of this peak in the ambient data, we expect that the oxidation of furan is a more likely source for this compound. This is further supported by laboratory work at Georgia Tech on the oxidation of 3-methylfuran by  $\text{NO}_3$ , in which a  $\text{C}_5\text{H}_5\text{NO}_5$  compound, likely a nitrooxy carbonyl, was observed to form in high yield.<sup>36</sup> In the RECAP data, we also observe a signal at  $m/z$  244 likely arising from a  $\text{C}_5\text{H}_5\text{NO}_5$  nitrooxy carbonyl from the oxidation of methylfurans. The ratio of the signal at  $m/z$  230 to  $m/z$  244 is typically 4:1. The source of furans in Los Angeles is likely a combination of biomass burning and cooking. Clearly, furan chemistry contributed significantly to the gas-phase nitrate chemistry in Pasadena in the summer of 2021 and the formation and loss of these compounds should be further investigated.

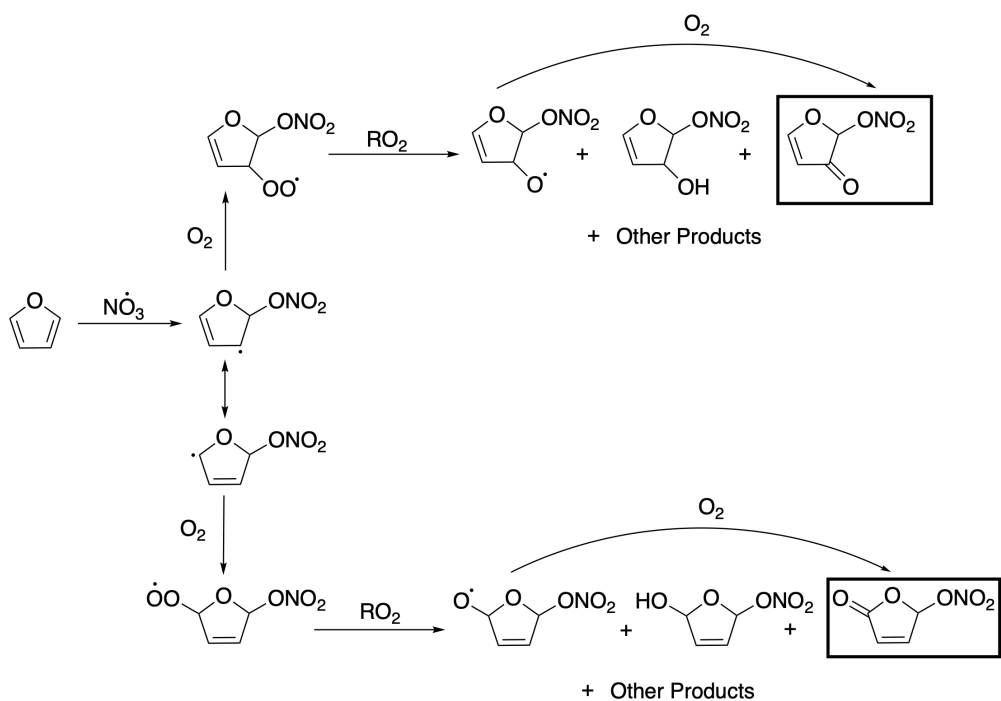


Figure 7: Possible mechanism for the formation of the carbonyl compound observed at  $m/z$  230 via oxidation of furan by  $\text{NO}_3$ .

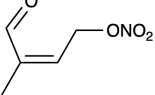
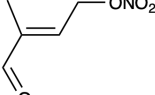
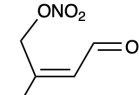
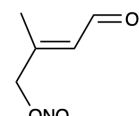
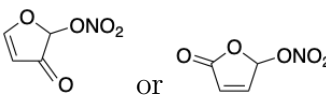
While the formation of nitrooxy carbonyls in the nighttime oxidation of monoterpenes is also theoretically possible, little to no signal at the mass of these compounds ( $m/z$  298) is observed in the ambient data. This is likely due to the fact that the majority of the monoterpene-derived peroxy radicals generated at night are tertiary peroxy radicals that cannot form the carbonyl<sup>7</sup> or that these peroxy radicals preferentially undergo autoxidation.<sup>34,37,38</sup>

### Nitrooxy Hydroperoxides

The nitrooxy hydroperoxides of isoprene, formed in the reaction of isoprene-derived  $n\text{RO}_2$  with  $\text{HO}_2$  (Reaction 8), are observed at  $m/z$  248.



Table 2: Assignments of chromatographic peaks observed in the ambient data at m/z 230. Peak numbers correspond to those peak numbers given in Figure 6.

Peak	Elution Temperature (°C)	Assignment
1	74.5	
2	77.3	
3	80.1	
4	88.7	
5	91.3	 or

To identify these compounds, we compare the elution temperatures of the ambient peaks at this mass to those formed in the dark oxidation of isoprene (Figure S4). At night, two of the major peaks observed in the ambient data have the same elution temperatures as the two nitrooxy hydroperoxides produced in  $\text{NO}_3$ -initiated oxidation of isoprene. However, several additional compounds are also observed at this mass, including compounds formed in the oxidation of C<sub>6</sub> alkenes (e.g., 2-methyl-2-pentene and n-hexenes) or hydroxynitrates produced via oxidation and subsequent H-shift chemistry of hexane. The overall concentration of compounds at this mass is approximately equal to the concentration of isoprene-derived hydroxy nitrates at night observed throughout the campaign (Figure SXX), suggesting that the reaction of nRO<sub>2</sub> with HO<sub>2</sub> may play an important role in this region at night.

## **Anthropogenic Nitrates**

### **Small Alkene-Derived Hydroxy Nitrates**

Hydroxy nitrates derived from alkenes are formed both in the daytime by OH oxidation and at night by  $\text{NO}_3$  oxidation. In our CIMS the smallest of these hydroxy nitrates, the ethene-derived hydroxy nitrate, is observed at  $m/z$  192. The larger alkene-derived hydroxy nitrates are then observed at  $m/z = 192 + (n \times 14)$ , where n is the number of additional  $\text{CH}_2$  groups. For hydroxy nitrates derived from  $\text{C}_4$  and  $\text{C}_5$  alkenes, the products of multiple precursor alkenes contribute to the signal at the corresponding  $m/z$ . These products were separated in the GC-CIMS, and were identified by comparison to the elution temperatures of hydroxy nitrates formed in the laboratory oxidation of various alkenes. Those compounds that we identified in the ambient data are given in Table 3, and the behavior of these individual compounds is discussed below.

The diurnal profiles of these small alkene-derived hydroxy nitrates are consistent with their formation primarily during the daytime (for example, Figure 3a, b, and e). Further, the signals at the masses of these hydroxy nitrates in the CToF-CIMS are well-correlated, consistent with a common source for the precursors of these compounds (Figure 8).

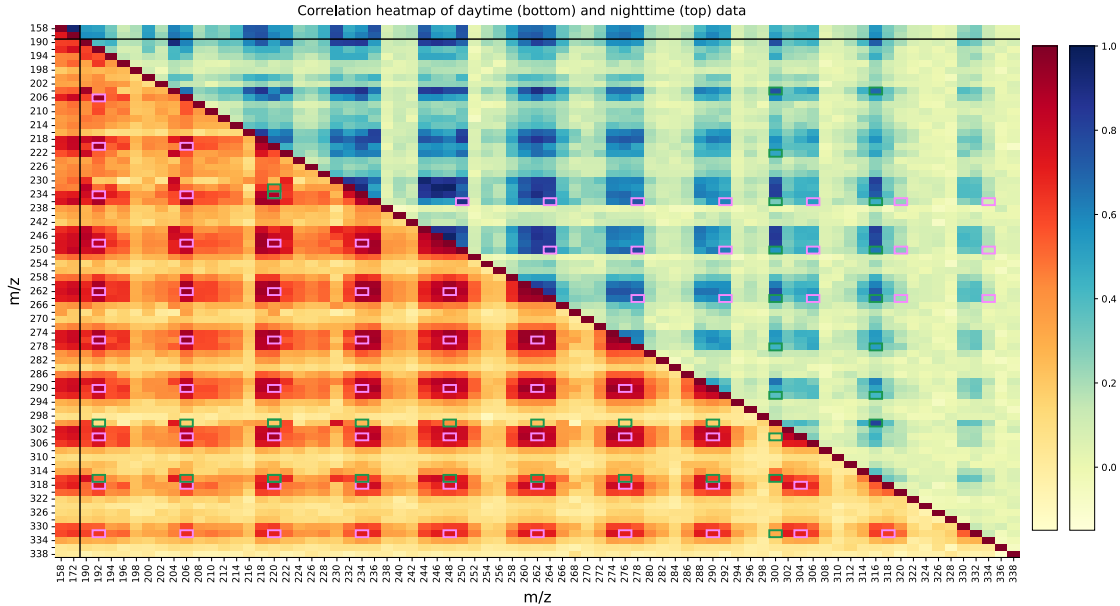
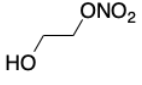
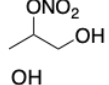
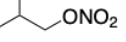
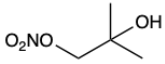
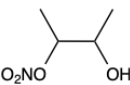
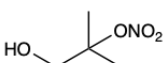
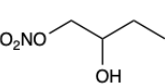
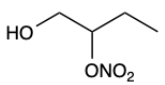
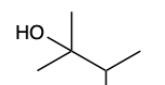
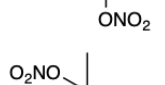
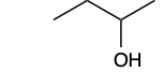
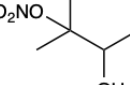
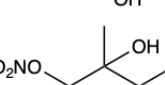
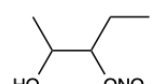
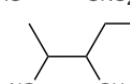
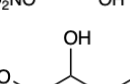
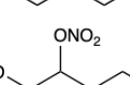
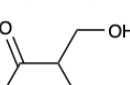
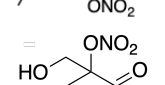


Figure 8: Correlation matrix for all even masses between  $m/z$  190 and  $m/z$  338.  $m/z$  158 and  $m/z$  172 are also included as the first two rows and are separated from the rest of the data by solid black lines. The lower left triangle shows the correlations during the daytime (warm colors) and the upper right triangle shows the correlations during the nighttime (cool colors). Pink boxes highlight the correlations between the masses in the  $m/z$   $192 + 14n$  series. Green boxes highlight correlations between masses that contain biogenic-derived nitrates. In this analysis, ‘daytime’ is defined as 8:00 AM - 5:00 PM and ‘nighttime’ is defined as 8:00 PM - 4:00 AM.

The relative production rates of a set of isomeric hydroxy nitrates during the daytime can be estimated by taking the sum of the products of the observed concentrations of the parent alkenes,<sup>33</sup> their rate constants with OH, and the nitrate yields from Reaction 4a. Figure 9 shows that the relative signals at the masses of these small alkene-derived hydroxy nitrates are generally consistent with this estimate of their relative production rates. The composition of the signal at each mass, however, consists of a diversity of compounds, and therefore a detailed picture of the overall chemistry requires chromatographic separation.

Table 3: Assignments of ambient chromatographic peaks that correspond to hydroxy nitrates derived from small alkenes.

m/z	Elution Temperature (°C)	Assignment
192	48.1	
206	46.8	
	52.0	
220	45.5	
	52.6	
58.1		
		
65.0		
		
72.9		
		
234	49.8	
	61.3	
64.4		
		
69.1		
		
72.1		
		
82.1		
		
87.5		
		
90.2		
100.3		

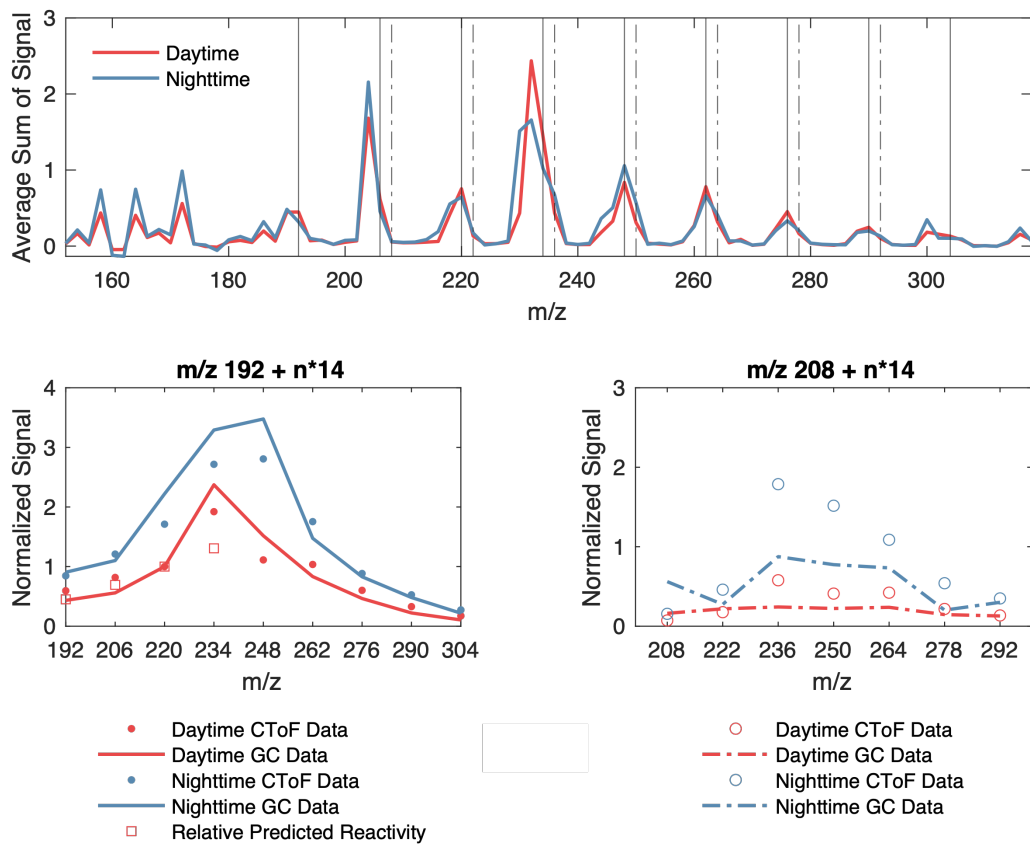


Figure 9: Comparison of the average relative sums of the normalized signals over the time period between August 28th, 2021 and September 5th, 2021 for the GC-HRToF (lines) and CToF-CIMS (circles) at each of the small alkene-derived hydroxy nitrate masses (lower left panel) and the small alkene-derived nitrooxy hydroperoxide masses (lower right panel) during both the daytime (red) and the nighttime (blue). Signals are given relative to the sum of the signal at the  $m/z$  220. The open squares in the lower left panel show the relative predicted reactivities, calculated as described in the text. Note that the discrepancy in the average sum of the signal across the CToF and GCToF in the hydroperoxide series is due to low transmission of these compounds in the 2m GC. The upper panel shows the average sum of the CToF-CIMS signal at all masses between  $m/z$  152 and  $m/z$  318 during the daytime (red) and nighttime (blue) between August 28th, 2021 and September 5th, 2021. Solid vertical lines denote masses in the hydroxy nitrate series ( $m/z$  192 +  $n^*14$ ) and dashed vertical lines denote the masses in the hydroxy hydroperoxide series ( $m/z$  208 +  $n^*14$ ).

The reactions of ethene and propene with OH and  $\text{NO}_3$  produce one isomer of a C2 hydroxy nitrate at  $m/z$  192 and two isomers of a C3 hydroxy nitrate at  $m/z$  206, respectively. The compounds observed at these masses in the ambient data have elution temperatures

consistent with these hydroxy nitrates as observed in laboratory oxidation data (Figures S2 and S3), with little to no contribution from compounds eluting at different temperatures. Therefore, we assign the entirety of the signal at m/z 192 to the ethene-derived hydroxy nitrate, and similarly that of m/z 206 is assigned to the propene-derived hydroxy nitrate. At m/z 206, the structural isomers of the propene-derived hydroxy nitrate are well separated and, as expected, the relative abundance of these isomers changes significantly as the dominant oxidant changes from OH during the daytime to NO<sub>3</sub> at night (both OH and NO<sub>3</sub> favor addition at the terminal carbon). In total, the nitrates produced from these two alkenes contribute (on average) a maximum of 7% to the total overall signal at even masses during the daytime and 3% at night.

The chromatographic signal at m/z 220, the mass consistent with hydroxy nitrates derived from C4 alkenes, is more complex (Figure 10). Laboratory oxidation experiments in the presence of OH/NO and/or NO<sub>3</sub> with 2-methylpropene, cis-2-butene, 1-butene, and butadiene as precursors were performed for comparison to the ambient data. Throughout the campaign, major contributions to this signal were consistent with hydroxynitrates produced from methylpropene and 1-butene during the daytime, with a more minor contribution from cis-2-butene-derived hydroxy nitrates. This is largely consistent with the relative emissions, rate constants, and nitrate yields of these three compounds with respect to reaction with OH. During the daytime, an additional prominent peak is observed at an elution temperature matching that of a nitrate formed in the oxidation of butadiene, along with another nitrate that elutes at approximately 90 °C (Figure 10).

During the nighttime, the contribution to the overall signal at m/z 220 is more evenly distributed across the various C4 hydroxy nitrate isomers. Although the tertiary hydroxy nitrate isomer of methylpropene (assigned to the peak eluting at approximately 45.5 °C) appears to be formed during the night, other compounds exhibit a diurnal behavior more consistent with formation during the daytime and persistence at night. This observation is consistent with the much higher predicted nighttime production rate of methylpropene-

derived nitrates as compared to other C4 alkenes. However, similarly to the daytime signal, there is a distinct compound observed at an elution temperature (87.6 °C) inconsistent with those of the hydroxy nitrates of the alkenes and with the butadiene-derived nitrates observed during the daytime. The elution temperature is consistent with a compound formed in the oxidation of 2-methylpropene that is not one of the hydroxy nitrates, but this compound remains unidentified. Overall, the signal at m/z 220 peaks at approximately noon at a concentration of 15 ppt, decreasing throughout the day to an average concentration of approximately 7 ppt at night. This corresponds to, on average, a maximum of 5% of the total signal at even masses during the daytime and a maximum of 3% of the total signal at even masses during the night. Despite the contributions to the signal from unidentified peaks, the production rate estimated from the alkenes relative to ethene matches their signal relative to ethene, suggesting that it is possible that these additional compounds are formed in the oxidation of C4 alkenes.

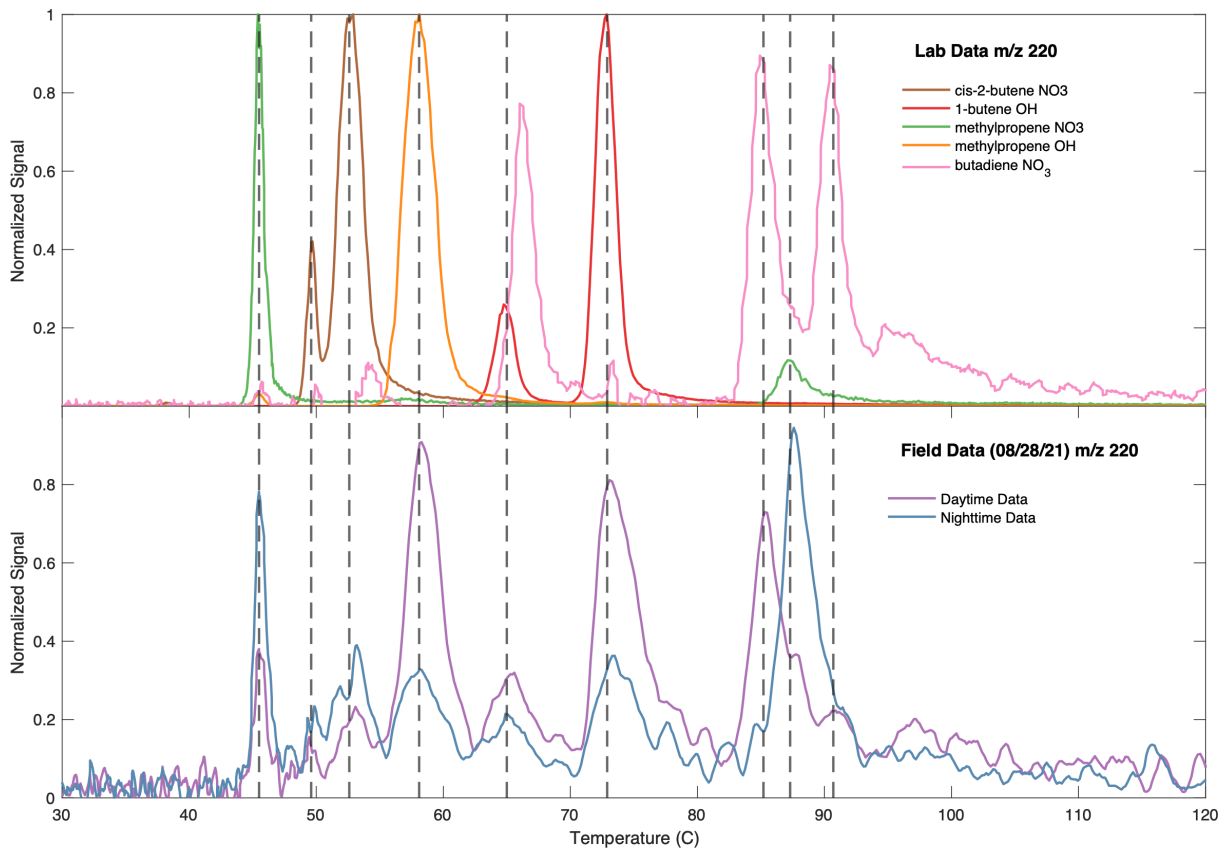


Figure 10: Ambient chromatographic data at m/z 220 (lower panel) from 08/28/2021 with daytime signal in purple and nighttime data in blue. Each trace in the lower panel is a sum of the traces during the daytime and nighttime period. Chromatographic data from a series of laboratory oxidation experiments (upper panel) are shown for comparison.

Hydroxy nitrates formed in the oxidation of C5 alkenes, C<sub>5</sub>NO<sub>4</sub>H<sub>11</sub> are observed at m/z 234. As mentioned previously, C<sub>4</sub>NO<sub>5</sub>H<sub>7</sub> carbonyl hydroxy nitrates formed from the 2nd generation isoprene oxidation products, are also observed at this mass, as are compounds formed in the oxidation of pentane by OH and subsequent hydrogen shifts. Laboratory oxidation experiments of 2-methyl-1-butene, 2-methyl-2-butene, 1-pentene, cis-2-pentene, pentane, MVK and MACR were performed for comparison to the ambient data (Figure 11). The proposed identities of the compounds observed in the ambient data at this mass are given in Table 3.

The oxidation of MVK by OH produces two major hydroxy nitrates in approximately

equal abundance which elute at 89.0 and 100.3°C. These correspond to hydroxy nitrates that form following OH addition at either the secondary or primary carbon, respectively, as labeled MVKN' and MVKN in Praske et al.<sup>5</sup> Although OH addition at the primary is favored, the nitrate yield is much lower as a result of the alpha carbonyl group. Praske determined that the total nitrate yield from MVK oxidation in the presence of NO is only 4% (2.4 and 1.6% for MVKN and MVKN', respectively). The oxidation of MACR by OH at high NO yield almost exclusively a hydroxy nitrate that elutes at 90.2°C. However, under typical concentrations of NO during the ambient measurements reported here, no MACR nitrate will be formed via this chemistry due to the rapid H-shift from the aldehyde to the tertiary peroxy radical.<sup>?</sup>

During the daytime and nighttime, GC signals at m/z 234 and the individual peaks at 90.2°C (MACRN) and 100.3°C (MVKN), we find that the C<sub>4</sub>NO<sub>5</sub>H<sub>7</sub> carbonyl hydroxy nitrates contribute, on average, approximately 49(±12)% of the total signal at m/z 234 during the daytime and 21(±8)% to the total signal at m/z 234 at night (Table SXX) with approximately equal contributions from each peak. Little to no signal corresponding to MVKN' is observed in the atmospheric chromatograms suggesting that the oxidation of MVK is not a major contributor to the formation of this nitrate. Rather, these data suggest that the source of this nitrate is mostly, if not entirely, from the oxidation of 4,3-IHN. This is entirely plausible given the fast reaction rate coefficient (4 × 10<sup>−11</sup>) and high yield of MVKN from the OH oxidation of 4,3-IHN (nearly 75%)<sup>26(?)</sup>. The source of the MACRN is less obvious - it certainly does not, however, originate from the OH-initiated oxidation of MACR. Wennberg et al.<sup>32</sup> suggested that the yield of MACRN from OH oxidation of 1,2-IHN was only 13% based on preliminary laboratory studies. The observed ratio of MACRN to MVKN is, however, higher than predicted by such a low yield. Either there are additional sources of MACRN, or the yield estimate from oxidation of 1,2-IHN is too low, the yield of MVKN is too high, or some combination of these.

In addition to MVKN and MACRN, there is significant production of the C<sub>5</sub>NO<sub>4</sub>H<sub>11</sub>

hydroxy nitrates derived from 2-methyl-1-butene, cis-2-pentene, and 1-pentene, with a small contribution to the signal from the hydroxy nitrates derived from 2-methyl-2-butene. Although not shown in the figure for simplicity, the hydroxy nitrates formed at m/z 234 in the OH-initiated oxidation of pentane elute at temperatures quite close to those produced in the oxidation of 1-pentene and MVK at 87.5°C and 90.2°C, respectively. Therefore, there is likely some contribution from the pentane OH products to the peaks observed at these elution temperatures in the ambient data. An additional unknown compound elutes during the daytime at approximately 78.8°C, inconsistent with the elution temperatures of compounds in any of the above oxidation experiments, but this contribution is relatively minor. Several of the alkene-derived hydroxy nitrates appear to either undergo secondary reaction or persist throughout the night, while there seems to be more significant nighttime production of the hydroxy nitrate derived from 2-methyl-1-butene.

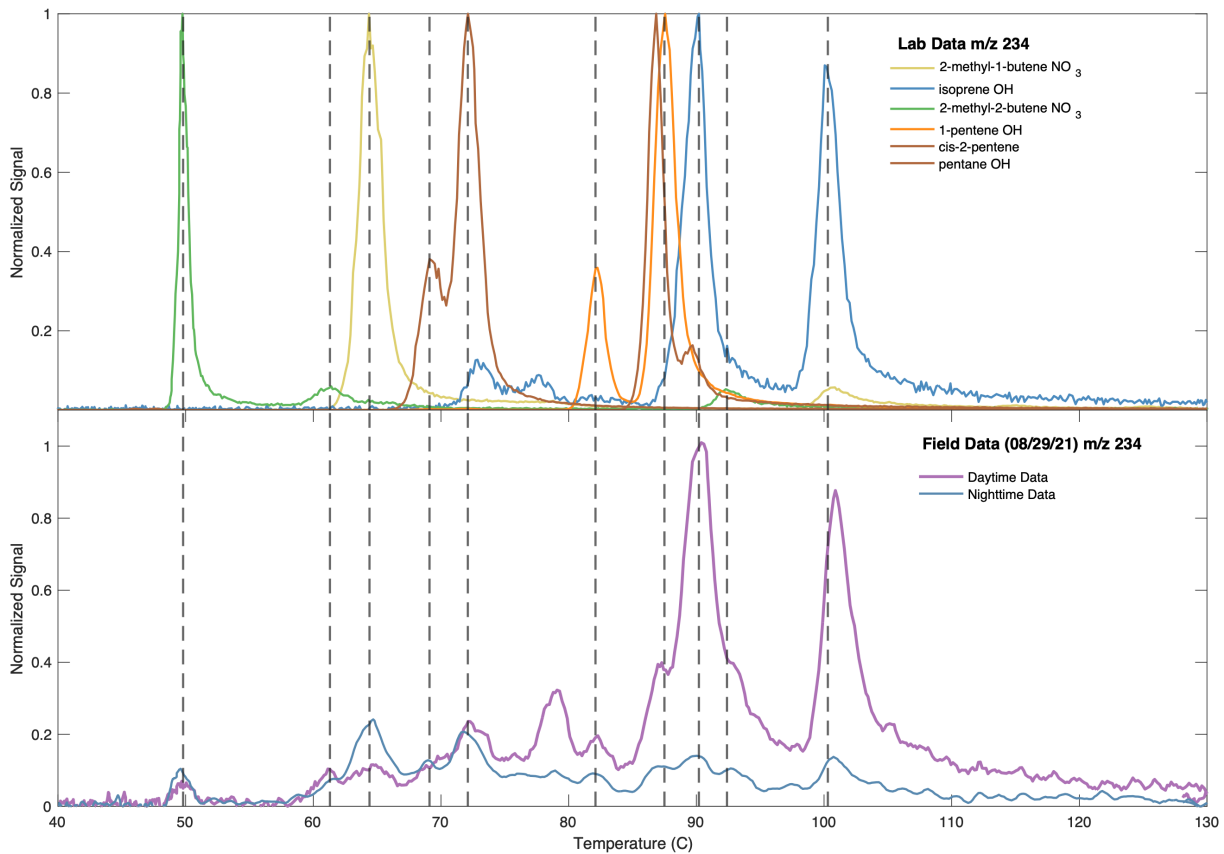


Figure 11: Ambient chromatographic data at m/z 234 (lower panel) from 08/29/2021 with daytime signal in purple and nighttime data in blue. Each trace in the lower panel is a sum of the traces during the daytime and nighttime period. Chromatographic data from a series of laboratory oxidation experiments (upper panel) are shown for comparison.

The overall signal at m/z 234 peaks at around noon at a concentration of approximately 25 ppt on average, decreasing throughout the day to a concentration of approximately 5 ppt at night. This corresponds to a maximum average contribution of 10% to the total signal at even m/z during the daytime and approximately 3% to the total signal at even m/z at night. This diurnal behavior is largely driven by the formation of the C<sub>4</sub>NO<sub>5</sub>H<sub>7</sub> nitrates, accounting for the discrepancy between the relative formation rate and relative signal observed in Figure 9. However, despite the importance these nitrates at m/z 234, there is still significant formation of C<sub>5</sub>NO<sub>4</sub>H<sub>11</sub> hydroxy nitrates via the reaction of several small C<sub>5</sub> alkenes, as can be seen in Figure 11.

## Nitrooxy Carbonyls

Nitrooxy carbonyls are formed primarily in the self reaction of nRO<sub>2</sub> or in the oxidation of hydroxy nitrates via abstraction of the hydrogen atom  $\alpha$  to the -OH group. These carbonyls appear at an m/z two less than that of the corresponding hydroxy nitrates. Table 4 gives the structures of the identified nitrooxy carbonyls formed in the oxidation of C2-C5 alkenes, which begin at m/z 190 and increase by 14 with each addition of a CH<sub>2</sub> group.

Table 4: Assignments for ambient peaks corresponding to nitrooxy carbonyls derived from small alkenes in the GC-CIMS. Note that where there are multiple isomers, assignments are speculative.

m/z	Elution Temperature (°C)	Assignment
204	41.9	
218	38.2	
54.3		
232	45.9	
	47.5	

No significant signal at the mass of the ethene-derived nitrooxy carbonyl (m/z 190) was observed in the ambient data. However, a prominent peak at the mass of a C3 nitrooxy carbonyl (m/z 204) is observed in the ambient data at an elution temperature of 41.9 °C. C3 nitrooxy carbonyls are formed both in the NO<sub>3</sub>-initiated oxidation of propene and the NO<sub>3</sub>-initiated oxidation of isoprene. The identity of the compound observed in the ambient data is assigned by comparison to the chromatograms of this mass observed in the NO<sub>3</sub>-initiated dark oxidation of propene. While there are two peaks at m/z 204 which appear in the dark oxidation of propene, one of which matches the elution temperature of the prominent

ambient peak at this mass and one of which matches the elution temperature of a more minor peak in the ambient data, only the more prominent peak is assigned to a C3 nitrooxy carbonyl (Table 4). These peaks appear to be the only contribution to the signal at m/z 204.

The ambient GC signal at m/z 218, the mass of C4 nitrooxy carbonyls in the CIMS, contains several prominent compounds present during both the daytime and the nighttime. Two of these compounds elute at temperatures corresponding to those of nitrooxy carbonyls formed in the  $\text{NO}_3$ -initiated oxidation of cis-2-butene ( $38.2\text{ }^\circ\text{C}$ ) and 1-butene ( $54.3\text{ }^\circ\text{C}$ ) and are assigned to these C4 nitrooxy carbonyls (Table 4). However, several of the compounds observed at m/z 218 in the ambient data exhibit diurnal behavior consistent with a unique daytime source, and are therefore likely not nitrooxy carbonyls. Two peaks observed in the ambient data, for example, correspond to the hydroxy nitrates formed in the oxidation of butadiene, with elution temperatures of  $66.3\text{ }^\circ\text{C}$  and  $90.4\text{ }^\circ\text{C}$ . However, the GC signal at m/z 218 is complex and several compounds, primarily a prominent peak at  $58.7\text{ }^\circ\text{C}$ , remain unidentified.

The overwhelming majority of the signal at m/z 232, the mass at which C5 alkene-derived nitrooxy carbonyls are observed, is composed of isoprene-derived hydroxy nitrates, as discussed in the previous section on biogenic nitrates. However, two small peaks observed in the nighttime ambient data at this mass elute at a temperature matching those of the nitrooxy carbonyls formed in the laboratory  $\text{NO}_3$ -initiated oxidation of cis-2-pentene ( $45.9\text{ }^\circ\text{C}$  and  $47.5\text{ }^\circ\text{C}$ ), and these ambient peaks are thus assigned to the two isomers of this nitrooxy carbonyl.

As described above, several small alkene-derived nitrooxy carbonyls are observed in this study (Table 4) and these compounds play a prominent role in the nitrate chemistry observed in the ambient atmosphere during the campaign.

## Nitrooxy Hydroperoxides

Small alkene-derived nitrooxy hydroperoxides are observed in the GC-CIMS at  $m/z = 208 + n \times 14$ , where  $m/z = 208$  is the mass of the ethene-derive nitrooxy hydroperoxide and  $n$  is the number of additional  $\text{CH}_2$  groups for each subsequent compound in the series. These hydroperoxides are produced at night in the reaction of nitrooxy peroxy radicals with  $\text{HO}_2$  (when  $\text{NO}$  levels are effectively zero due to titration by  $\text{O}_3$ ). Figure 9 shows that, while the formation of these compounds is less significant in the oxidation of C2 and C3 alkenes, their production appears to be more important in the oxidation of C4, C5, and C6 compounds, reflecting the higher  $\text{NO}_3$  reactivity of some of these compounds. Consistent with the observation that the signal at these masses is low for ethene- and propene-derived  $\text{nRO}_2$ , no clear peaks are observed at  $m/z$  208. At  $m/z$  222, we observe one primary peak that is present exclusively at night. This peak has an elution temperature consistent with the nitrooxy hydroperoxide formed in the laboratory oxidation of propene by  $\text{NO}_3$ , and is therefore assigned as such. The presence of only one peak suggests either that only the major addition of  $\text{NO}_3$  to form a secondary  $\text{nRO}_2$  is occuring at a significant rate or that the isomers of this compound are poorly separated. Due to the excellent separation of the hydroxy nitrate isomers observed at  $m/z$  206, this latter possibility seems unlikely. We therefore assign the peak at  $m/z$  220 to only one isomer, likely of that corresponding to the more abundant nighttime  $\text{nRO}_2$ .

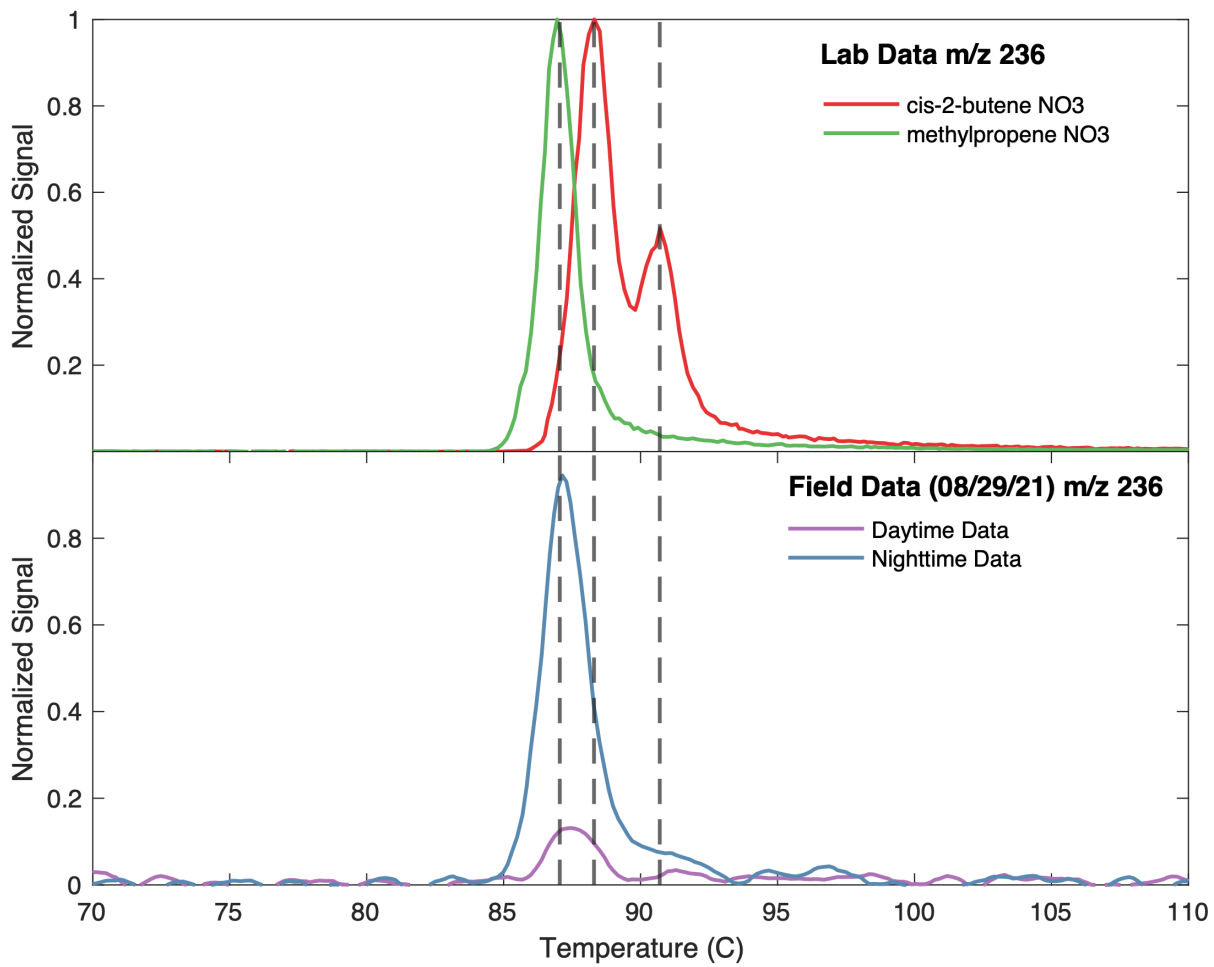
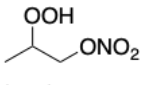
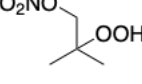
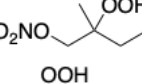
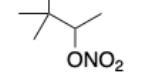


Figure 12: Ambient chromatographic data at  $m/z$  236 (lower panel) from 08/29/2021 with daytime signal in purple and nighttime data in blue. Each trace in the lower panel is a sum of the traces during the daytime and nighttime period. Chromatographic data from a series of laboratory oxidation experiments (upper panel) are shown for comparison.

At  $m/z$  236, the mass of the C4 alkene-derived nitrooxy hydroperoxide, we observe one primary peak in the ambient data eluting at 87.1°C. The identity of this compound is assigned to the methylpropene-derived nitrooxy hydroperoxide by comparison to our laboratory oxidation experiments (Figure 12). There is a small shoulder at higher temperature and a second peak at ~91°C that is suggestive of a small amount of nitrooxy hydroperoxides produced from the 2-butenes. Using the ratio of the abundance of 2-butenes and methylpropene from Van Rooy et al.<sup>33</sup> we calculate that the NO<sub>3</sub> reactivity with the cis- and trans-2-butenes

are about 20% of the reactivity with methylpropene. The prominence of methylpropene-derived nighttime nRO<sub>2</sub> chemistry is consistent with several other observations of significant contributions of methylpropene-derived nitrates in this study — this general prominence of nighttime methylpropene chemistry is due to a combination of its much higher abundance and as fast, if not faster, reactivity than the other C4 alkenes.

Table 5: Assignments for peaks corresponding to nitrooxy hydroperoxides derived from small alkenes in the GC-CIMS. Note that where multiple isomers are possible the assignments are speculative.

m/z	Elution Temperature	Assignment
222	85.0	
236	87.1	
250	92.0	
	100.2	

Finally, three peaks are observed in the ambient chromatographic data at m/z 250, the mass corresponding to C5 nitrooxy hydroperoxides. Two of these peaks are significantly more prominent than the third (Figure 13). By comparison to the elution temperatures of nitrooxy hydroperoxides formed in the laboratory oxidation of 2-methyl-2-butene and 2-methyl-1-butene, we assign these peaks to the nitrooxy hydroperoxides derived from these compounds (Table 5). The identity of the third peak is currently unknown. However, the high concentrations of the 2-methyl-2-butene and 2-methyl-1-butene-derived nitrooxy hydroperoxides suggest that the nRO<sub>2</sub> of these precursor alkenes undergo significant reaction with HO<sub>2</sub> at night throughout the campaign.

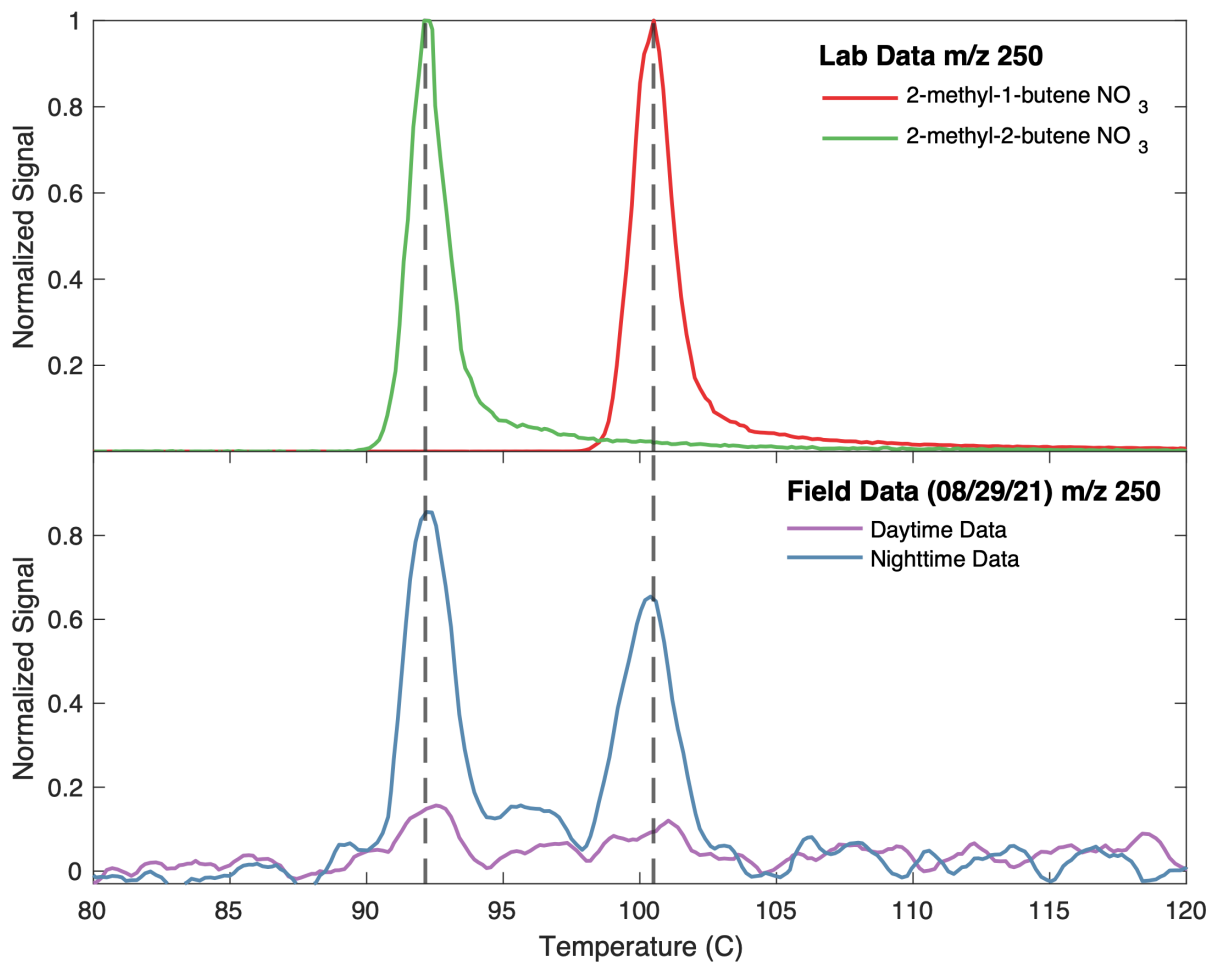


Figure 13: Ambient chromatographic data at m/z 250 (lower panel) from 08/29/2021 with daytime signal in purple and nighttime data in blue. Each trace in the lower panel is a sum of the traces during the daytime and nighttime period. Chromatographic data from a series of laboratory oxidation experiments (upper panel) are shown for comparison.

## Nitroaromatics

A significant contribution to the total nitrogen-containing organic compounds is observed at the mass corresponding to nitroaromatics. Nitroaromatics are primarily formed in the atmospheric oxidation of benzene and other aromatic compounds such as toluene and catechol in the presence of NO<sub>2</sub>. These nitroaromatics generally undergo a fluorine transfer reaction in our GC-CIMS and thus are observed at  $m/z = mw + 19$ . For example, nitrophenol, which has a molecular weight of 139, is observed at m/z 158. The formation of these nitroaromatic

compounds has been shown to play a significant role in urban chemistry in other areas with high NO<sub>x</sub> and significant anthropogenic VOC emissions.<sup>39</sup> In our data, a signal at m/z 158 is observed in both the GC-CIMS and in the CToF-CIMS equal to the signal observed at m/z 220 during the time period discussed here (Figure SXX). The identity of the ambient chromatographic peak observed at m/z 158 was confirmed by comparison of the chromatography to that of a 2-nitrophenol standard present in the hot calibration system of the GC-CIMS. The signal at m/z 172, corresponding to addition of OH and NO<sub>2</sub> to toluene, is of similar magnitude. The sum of the signal at m/z 158 and m/z 172 contributes up to 10% of the total signal at even m/z observed on average. Therefore, along with small alkene-derived chemistry, nitroaromatic compounds make a significant contribution to the anthropogenic nitrate chemistry observed during the campaign.

## Nitrate Aerosol

Aerosol Mass Spectrometer measurements were also taken during the time period discussed here to determine the composition of the ambient fine particulate matter (PM 1.0). As in previous studies the ratio of this ion to that ion is used to estimate the fraction of organic aerosol containing nitrogen. Figure 14 shows that the organic nitrate aerosol is most significant during the nighttime, reaching an average concentration of approximately 0.18  $\mu\text{g}/\text{m}^3$  at night. The concentration then rapidly decreases at approximately noon, rising again at approximately 8 PM.

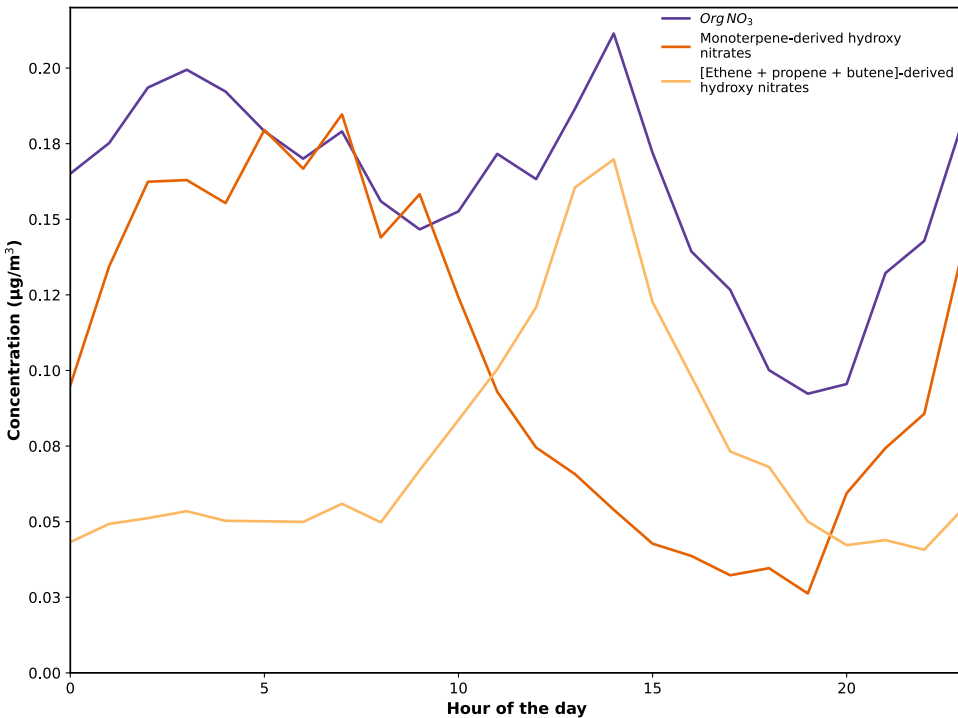


Figure 14: Diurnal profiles of total particulate organic nitrate (purple), monoterpane-derived particulate nitrate (red, the sum of m/z 300 and 316 scaled up by a factor of five) and alkene-derived particulate nitrate (yellow) measured with the AMS during this time period.

The increase of the organic nitrate aerosol concentration at 8 PM is consistent with the partitioning of organic nitrates to the aerosol phase formed via nighttime chemistry. These low volatility compounds are likely formed following the reaction of  $\text{NO}_3$  with mono and sesquiterpenes, which have been shown in the laboratory to lead to secondary organic aerosol. Additions from reactions with other large alkenes are likely also important. Consistent with this hypothesis, the concentration of organic nitrogen in the aerosol coincides with the steep rise in m/z 300 and 316 after sunset (Figure 3).

As shown in Figure 14, there is also a daytime source of aerosol organic nitrogen that follows the increase in the concentrations of small hydroxy nitrates. This behavior is consistent with the formation of low volatility alkyl nitrates produced with OH chemistry—likely produced from larger VOCs.

Together, the amount of organic nitrogen present on PM 1.0 is approximately equal to

the sum of m/z 300, 316, 192, 206 and 220. This represents about xx % of the sum of all alkynitrates.

## Conclusion

The census of multifunctional organic nitrates observed during the RECAP-CA field campaign in Pasadena in the summer of 2021 provides a measure of which VOCs contribute to the formation of ozone and organic aerosol. Biogenic (largely isoprene-derived) and anthropogenic hydrocarbons play similar roles in the overall organic nitrate chemistry during the time period examined here, with significant contributions to the anthropogenic nitrate budget from both small alkenes and aromatic compounds such as benzene and toluene. Furan-derived nitrooxy carbonyls are a major nighttime reservoir of organic nitrogen. Further, the small alkene-derived nitrates are well-correlated with each other, consistent with a common source. The ratio of the measured concentrations of these nitrates are well-predicted by their production rates estimated from previous measurements of the ratios of the concentrations of the parent alkenes. Finally, both biogenic and anthropogenic VOCs contribute to the formation of nitrogen-containing organic aerosols.

## References

- (1) Beaver, M. R.; Clair, J. M. S.; Paulot, F.; Spencer, K. M.; Crounse, J. D.; LaFranchi, B. W.; Min, K. E.; Pusede, S. E.; Wooldridge, P. J.; Schade, G. W.; Park, C.; Cohen, R. C.; Wennberg, P. O. Importance of biogenic precursors to the budget of organic nitrates: observations of multifunctional organic nitrates by CIMS and TD-LIF during BEARPEX 2009. *Atmospheric Chemistry and Physics* **2012**, *12*, 5773–5785, Publisher: Copernicus GmbH.

- (2) Zhang, J. J.; Wei, Y.; Fang, Z. Ozone Pollution: A Major Health Hazard Worldwide. *Frontiers in Immunology* **2019**, *10*, Publisher: Frontiers.
- (3) Teng, A. P.; Crounse, J. D.; Lee, L.; St. Clair, J. M.; Cohen, R. C.; Wennberg, P. O. Hydroxy nitrate production in the OH-initiated oxidation of alkenes. *Atmospheric Chemistry and Physics* **2015**, *15*, 4297–4316, Publisher: Copernicus GmbH.
- (4) Perring, A. E.; Pusede, S. E.; Cohen, R. C. An Observational Perspective on the Atmospheric Impacts of Alkyl and Multifunctional Nitrates on Ozone and Secondary Organic Aerosol. *Chemical Reviews* **2013**, *113*, 5848–5870, Publisher: American Chemical Society.
- (5) Praske, E.; Crounse, J. D.; Bates, K. H.; Kurtén, T.; Kjaergaard, H. G.; Wennberg, P. O. Atmospheric Fate of Methyl Vinyl Ketone: Peroxy Radical Reactions with NO and HO<sub>2</sub>. *The Journal of Physical Chemistry A* **2015**, *119*, 4562–4572, Publisher: American Chemical Society.
- (6) Xu, L.; Møller, K. H.; Crounse, J. D.; Kjaergaard, H. G.; Wennberg, P. O. New Insights into the Radical Chemistry and Product Distribution in the OH-Initiated Oxidation of Benzene. *Environmental Science & Technology* **2020**, *54*, 13467–13477, Publisher: American Chemical Society.
- (7) Hallquist, M.; Wängberg, I.; Ljungström, E.; Barnes, I.; Becker, K.-H. Aerosol and Product Yields from NO<sub>3</sub> Radical-Initiated Oxidation of Selected Monoterpenes. *Environmental Science & Technology* **1999**, *33*, 553–559, Publisher: American Chemical Society.
- (8) Fry, J. L.; Kiendler-Scharr, A.; Rollins, A. W.; Wooldridge, P. J.; Brown, S. S.; Fuchs, H.; Dubé, W.; Mensah, A.; dal Maso, M.; Tillmann, R.; Dorn, H.-P.; Brauers, T.; Cohen, R. C. Organic nitrate and secondary organic aerosol yield from NO<sub>3</sub> oxidation

- of -pinene evaluated using a gas-phase kinetics/aerosol partitioning model. *Atmospheric Chemistry and Physics* **2009**, *9*, 1431–1449, Publisher: Copernicus GmbH.
- (9) Rollins, A. W.; Pusede, S.; Wooldridge, P.; Min, K.-E.; Gentner, D. R.; Goldstein, A. H.; Liu, S.; Day, D. A.; Russell, L. M.; Rubitschun, C. L.; Surratt, J. D.; Cohen, R. C. Gas/particle partitioning of total alkyl nitrates observed with TD-LIF in Bakersfield. *Journal of Geophysical Research: Atmospheres* **2013**, *118*, 6651–6662, eprint: <https://onlinelibrary.wiley.com/doi/pdf/10.1002/jgrd.50522>.
- (10) Schwantes, R. H.; Teng, A. P.; Nguyen, T. B.; Coggon, M. M.; Crounse, J. D.; St. Clair, J. M.; Zhang, X.; Schilling, K. A.; Seinfeld, J. H.; Wennberg, P. O. Isoprene NO<sub>3</sub> Oxidation Products from the RO<sub>2</sub> + HO<sub>2</sub> Pathway. *The Journal of Physical Chemistry A* **2015**, *119*, 10158–10171, Publisher: American Chemical Society.
- (11) Schwantes, R. H.; Charan, S. M.; Bates, K. H.; Huang, Y.; Nguyen, T. B.; Mai, H.; Kong, W.; Flagan, R. C.; Seinfeld, J. H. Low-volatility compounds contribute significantly to isoprene secondary organic aerosol (SOA) under high-NO<sub>x</sub> conditions. *Atmospheric Chemistry and Physics* **2019**, *19*, 7255–7278, Publisher: Copernicus GmbH.
- (12) Day, D. A.; Liu, S.; Russell, L. M.; Ziemann, P. J. Organonitrate group concentrations in submicron particles with high nitrate and organic fractions in coastal southern California. *Atmospheric Environment* **2010**, *44*, 1970–1979.
- (13) Fry, J. L. et al. Observations of gas- and aerosol-phase organic nitrates at BEACHON-RoMBAS 2011. *Atmospheric Chemistry and Physics* **2013**, *13*, 8585–8605, Publisher: Copernicus GmbH.
- (14) Lee, B. H. et al. Highly functionalized organic nitrates in the southeast United States: Contribution to secondary organic aerosol and reactive nitrogen budgets. *Proceedings of the National Academy of Sciences* **2016**, *113*, 1516–1521, Publisher: Proceedings of the National Academy of Sciences.

- (15) Rollins, A. W.; Browne, E. C.; Min, K.-E.; Pusede, S. E.; Wooldridge, P. J.; Gentner, D. R.; Goldstein, A. H.; Liu, S.; Day, D. A.; Russell, L. M.; Cohen, R. C. Evidence for NO<sub>x</sub> Control over Nighttime SOA Formation. *Science* **2012**, *337*, 1210–1212, Publisher: American Association for the Advancement of Science.
- (16) Vasquez, K. T.; Allen, H. M.; Crounse, J. D.; Praske, E.; Xu, L.; Noelscher, A. C.; Wennberg, P. O. Low-pressure gas chromatography with chemical ionization mass spectrometry for quantification of multifunctional organic compounds in the atmosphere. *Atmospheric Measurement Techniques* **2018**, *11*, 6815–6832.
- (17) Hyttinen, N.; Otkjær, R. V.; Iyer, S.; Kjaergaard, H. G.; Rissanen, M. P.; Wennberg, P. O.; Kurtén, T. Computational Comparison of Different Reagent Ions in the Chemical Ionization of Oxidized Multifunctional Compounds. *The Journal of Physical Chemistry A* **2018**, *122*, 269–279, Publisher: American Chemical Society.
- (18) Allen, H. M.; Bates, K. H.; Crounse, J. D.; Kim, M. J.; Teng, A. P.; Ray, E. A.; Wennberg, P. O. H<sub>2</sub>O<sub>2</sub> and CH<sub>3</sub>OOH (MHP) in the Remote Atmosphere: 2. Physical and Chemical Controls. *Journal of Geophysical Research: Atmospheres* **2022**, *127*, e2021JD035702, \_eprint: <https://onlinelibrary.wiley.com/doi/pdf/10.1029/2021JD035702>.
- (19) Allen, H. M.; Crounse, J. D.; Kim, M. J.; Teng, A. P.; Ray, E. A.; McKain, K.; Sweeney, C.; Wennberg, P. O. H<sub>2</sub>O<sub>2</sub> and CH<sub>3</sub>OOH (MHP) in the Remote Atmosphere: 1. Global Distribution and Regional Influences. *Journal of Geophysical Research: Atmospheres* **2022**, *127*, e2021JD035701, \_eprint: <https://onlinelibrary.wiley.com/doi/pdf/10.1029/2021JD035701>.
- (20) Xu, L. et al. Ozone chemistry in western U.S. wildfire plumes. *Science Advances* **2021**, *7*, eabl3648, Publisher: American Association for the Advancement of Science.
- (21) Middlebrook, A. M.; Bahreini, R.; Jimenez, J. L.; Canagaratna, M. R. Evaluation of

- Composition-Dependent Collection Efficiencies for the Aerodyne Aerosol Mass Spectrometer using Field Data. *Aerosol Science and Technology* **2012**, *46*, 258–271, Publisher: Taylor & Francis eprint: <https://doi.org/10.1080/02786826.2011.620041>.
- (22) Canagaratna, M. R.; Jimenez, J. L.; Kroll, J. H.; Chen, Q.; Kessler, S. H.; Massoli, P.; Hildebrandt Ruiz, L.; Fortner, E.; Williams, L. R.; Wilson, K. R.; Surratt, J. D.; Donahue, N. M.; Jayne, J. T.; Worsnop, D. R. Elemental ratio measurements of organic compounds using aerosol mass spectrometry: characterization, improved calibration, and implications. *Atmospheric Chemistry and Physics* **2015**, *15*, 253–272, Publisher: Copernicus GmbH.
- (23) Farmer, D. K.; Matsunaga, A.; Docherty, K. S.; Surratt, J. D.; Seinfeld, J. H.; Ziemann, P. J.; Jimenez, J. L. Response of an aerosol mass spectrometer to organonitrates and organosulfates and implications for atmospheric chemistry. *Proceedings of the National Academy of Sciences* **2010**, *107*, 6670–6675, Publisher: Proceedings of the National Academy of Sciences.
- (24) Xu, L. et al. Effects of anthropogenic emissions on aerosol formation from isoprene and monoterpenes in the southeastern United States. *Proceedings of the National Academy of Sciences* **2015**, *112*, 37–42, Publisher: Proceedings of the National Academy of Sciences.
- (25) Nguyen, T. B.; Crounse, J. D.; Schwantes, R. H.; Teng, A. P.; Bates, K. H.; Zhang, X.; St. Clair, J. M.; Brune, W. H.; Tyndall, G. S.; Keutsch, F. N.; Seinfeld, J. H.; Wennberg, P. O. Overview of the Focused Isoprene eXperiment at the California Institute of Technology (FIXCIT): mechanistic chamber studies on the oxidation of biogenic compounds. *Atmospheric Chemistry and Physics* **2014**, *14*, 13531–13549, Publisher: Copernicus GmbH.
- (26) Lee, L.; Teng, A. P.; Wennberg, P. O.; Crounse, J. D.; Cohen, R. C. On Rates and

Mechanisms of OH and O<sub>3</sub> Reactions with Isoprene-Derived Hydroxy Nitrates. *The Journal of Physical Chemistry A* **2014**, *118*, 1622–1637, Publisher: American Chemical Society.

- (27) Kwan, A. J.; Chan, A. W. H.; Ng, N. L.; Kjaergaard, H. G.; Seinfeld, J. H.; Wennberg, P. O. Peroxy radical chemistry and OH radical production during the NO<sub>3</sub>-initiated oxidation of isoprene. *Atmospheric Chemistry and Physics* **2012**, *12*, 7499–7515, Publisher: Copernicus GmbH.
- (28) Paulot, F.; Crounse, J. D.; Kjaergaard, H. G.; Kroll, J. H.; Seinfeld, J. H.; Wennberg, P. O. Isoprene photooxidation: new insights into the production of acids and organic nitrates. *Atmospheric Chemistry and Physics* **2009**, *9*, 1479–1501, Publisher: Copernicus GmbH.
- (29) Pfannerstill, E. Y.; Arata, C.; Zhu, Q.; Schulze, B. C.; Ward, R.; Woods, R.; Harkins, C.; Schwantes, R. H.; Seinfeld, J. H.; Bucholtz, A.; Cohen, R. C.; Goldstein, A. H. Temperature-dependent emissions dominate aerosol and ozone formation in Los Angeles. *Science* **2024**, *384*, 1324–1329, Publisher: American Association for the Advancement of Science.
- (30) Vasquez, K. T.; Crounse, J. D.; Schulze, B. C.; Bates, K. H.; Teng, A. P.; Xu, L.; Allen, H. M.; Wennberg, P. O. Rapid hydrolysis of tertiary isoprene nitrate efficiently removes NO<sub>x</sub> from the atmosphere. *Proceedings of the National Academy of Sciences* **2020**, *117*, 33011–33016, Publisher: Proceedings of the National Academy of Sciences.
- (31) Teng, A. P.; Crounse, J. D.; Wennberg, P. O. Isoprene Peroxy Radical Dynamics. *Journal of the American Chemical Society* **2017**, *139*, 5367–5377, Publisher: American Chemical Society.
- (32) Wennberg, P. O.; Bates, K. H.; Crounse, J. D.; Dodson, L. G.; McVay, R. C.; Mertens, L. A.; Nguyen, T. B.; Praske, E.; Schwantes, R. H.; Smarte, M. D.;

- St Clair, J. M.; Teng, A. P.; Zhang, X.; Seinfeld, J. H. Gas-Phase Reactions of Isoprene and Its Major Oxidation Products. *Chemical Reviews* **2018**, *118*, 3337–3390, Publisher: American Chemical Society.
- (33) Van Rooy, P.; Tasnia, A.; Barletta, B.; Buenconsejo, R.; Crounse, J. D.; Kenseth, C. M.; Meinardi, S.; Murphy, S.; Parker, H.; Schulze, B.; Seinfeld, J. H.; Wennberg, P. O.; Blake, D. R.; Barsanti, K. C. Observations of Volatile Organic Compounds in the Los Angeles Basin during COVID-19. *ACS Earth and Space Chemistry* **2021**, *5*, 3045–3055, Publisher: American Chemical Society.
- (34) Ng, N. L. et al. Nitrate radicals and biogenic volatile organic compounds: oxidation, mechanisms, and organic aerosol. *Atmospheric chemistry and physics* **2017**, *17*, 2103–2162.
- (35) Tuazon, E. C.; Alvarado, A.; Aschmann, S. M.; Atkinson, R.; Arey, J. Products of the Gas-Phase Reactions of 1,3-Butadiene with OH and NO<sub>3</sub> Radicals. *Environmental Science & Technology* **1999**, *33*, 3586–3595, Publisher: American Chemical Society.
- (36) Joo, T.; Rivera-Rios, J. C.; Takeuchi, M.; Alvarado, M. J.; Ng, N. L. Secondary Organic Aerosol Formation from Reaction of 3-Methylfuran with Nitrate Radicals. *ACS Earth and Space Chemistry* **2019**, *3*, 922–934, Publisher: American Chemical Society.
- (37) Berndt, T.; Richters, S.; Jokinen, T.; Hyttinen, N.; Kurtén, T.; Otkjær, R. V.; Kjaergaard, H. G.; Stratmann, F.; Herrmann, H.; Sipilä, M.; Kulmala, M.; Ehn, M. Hydroxyl radical-induced formation of highly oxidized organic compounds. *Nature Communications* **2016**, *7*, 13677, Publisher: Nature Publishing Group.
- (38) Nah, T.; Sanchez, J.; Boyd, C. M.; Ng, N. L. Photochemical Aging of -pinene and -pinene Secondary Organic Aerosol formed from Nitrate Radical Oxidation. *Environmental Science & Technology* **2016**, *50*, 222–231, Publisher: American Chemical Society.

- (39) Wang, Y. et al. The formation of nitro-aromatic compounds under high NO<sub>x</sub> and anthropogenic VOC conditions in urban Beijing, China. *Atmospheric Chemistry and Physics* **2019**, *19*, 7649–7665, Publisher: Copernicus GmbH.